

Preparation and Spectrophotometric Study of 2[2-(5-bromo thiazolyl) azo]-4-methoxy phenol

Arshed Abd Ali Shihad

Submitted to the
Institute of Graduate Studies and Research
in partial fulfillment of the requirements for the Degree of

Master of Science
in
Chemistry

Eastern Mediterranean University
June 2013
Gazimağusa, North Cyprus

Approval of the Institute of Graduate Studies and Research

Prof. Dr. Elvan Yılmaz
Director

I certify that this thesis satisfies the requirements as a thesis for the degree of Master of Science in Chemistry.

Prof. Dr. Mustafa Halilsoy
Chair, Department of Chemistry

We certify that we have read this thesis and that in our opinion it is fully adequate in scope and quality as a thesis for the degree of Master of Science in Chemistry

Asst. Prof. Dr. Mehmet U. Garip
Supervisor

Examining Committee

1. Prof. Dr. Elvan Yılmaz
2. Assoc. Prof. Dr. Mustafa Gazi
3. Asst. Prof. Dr. Mehmet Garip

ABSTRACT

A new thiazolylazo dye 2[2-(5-bromo thiazolyl) azo]-4-methoxy phenol (BrTAMP) was prepared by coupling reaction between 5-bromo thiazolylazonium chloride with 4-methoxy phenol in alkaline alcoholic solution. The structure of azo ligand has been characterized by Mass spectrometry, ¹HNMR, UV-visible and FT-IR spectrophotometry. Three new complexes of Cu (II), Ni (II) and Ag (I) ions were prepared and identified by UV-visible spectroscopy, molar conductivity measurement, and FT-IR spectroscopy. The spectral and analytical data show that the reagent is tridentate and coordination with metal ions are: (i) the azo N atom which adjacent to methoxy phenol radical, (ii) thiazole N atom and (iii) the phenolate O atom.

The metal ligand ratio (M:L) in alcoholic aqueous solutions determined by the “mole ratio” method and by Jobe's method, both indicate 1:2 for Cu (II) and Ni (II) complexes and 1:1 for Ag (I) complex. Stability constants for the complexes were also calculated from spectrophotometric data.

While octahedral configuration is suggested for Ni (II) and Cu (II) complexes, tetrahedral is suggested for Ag (I) complex. The solid complexes are found to have the general formula [ML₂].H₂O where M = Cu (II) or Ni (II) ions and [ML. H₂O] where M = Ag (I) ion. The analytical applications using the ligand to determine Cu (II) in a sample of human blood and Ni (II) in a sample of water from the Euphrates River were carried out.

Keywords: Thiazolylazo Ligand, Coupling Reaction, Metal Complexes, Characterization and Analytical Application

ÖZ

Yeni bir tiazolilazo boyar madde olan 2 [2 - (5-bromo tiazolil) azo]-4-metoksi fenol (BrTAMP), alkali alkollü çözücü içinde 4-metoksi fenol ile 5-bromo tiazolilazonium klorürün birleştirme reaksiyonu ile hazırlandı. Azo ligandın yapısı Kütle spektrumu, ¹HNMR, UV-görünür ve FT-IR gibi teknikleri ile karakterize edilmiştir. Cu (II), Ni (II) ve Ag (I) iyonlarının üç yeni kompleksleri hazırlandı ve UV-görünür spektroskopi, molar iletkenlik ölçümü, FT-IR spektrumları ile tanımlandı. Spektral ve analitik veriler, reaktifin üç dişli olduğunu, ve metal iyonuna koordinasyonun (i) metoksi fenol radikaline en yakın azo N atomu, (ii) tiazol N atomu ve (iii) fenolatın O atomu tarafından yapıldığını göstermektedir.

Mol oranı ve Jobe yöntemleri ile elde edilen analitik veriler alkollü su içerisinde çözülmüş komplekslerdeki metal iyonu ile reaktif oranının Cu (II) ve Ni (II) için 1:2, ve Ag (I) için 1:1 olduğunu göstermektedir. Komplekslerin kararlılık sabitleri de ayrıca spektrofotometrik veriler kullanılarak hesaplanmıştır.

Ni (II) ve Cu (II) kompleksleri için oktahedral yapı önerilirken, Ag (I) için önerilen yapı tetrahedraldır. Komplekslerin katı hallerinde aşağıdaki genel formüle sahip oldukları tespit edilmiştir: Cu (II) ve Ni (II) için [ML₂].H₂O, ve Ag(I) için [ML].H₂O. Reaktif (ligand) ile insan kanı örneğinde Cu (II), Fırat nehrinden alınan su örneğinde Ni (II) ve diş dolgu malzemesinde Ag (I) iyonlarının nicel analizi yapılmıştır.

Anahtar Kelimeler: Tiazolilazo Ligand, Bağlanma Reaksiyonu, Meta Kompleksleri, Karakterizasyon ve Analitik uygulamalar

ACKNOWLEDGMENTS

I am heartily thankful to my ideal thesis supervisor, Assist Prof. Dr. Mehmet U. Garip, whose sage advice, patient encouragement, guidance and steadfast support from the initial to the final level, aided the writing of this thesis in innumerable ways. One simply could not wish for a better or friendlier supervisor.

I would also like to express my sincere thanks to Prof. Dr. Khalid J. Al-Adilee for his unselfish advice and unfailing support as my co-supervisor and tutor.

Lastly, I offer my regards to my family who always supported and helped me to overcome the problems and difficulties.

TABLE OF CONTENTS

ABSTRACT.....	iii
ÖZ.....	iv
ACKNOLEDMENTS.....	v
LIST OF FIGURES.....	x
LIST OF SCHEMES.....	xii
LIST OF TABLES.....	xiii
1 INTRODUCTION.....	1
1.1 Azo Dyes.....	1
1.2 Classification of Azo Dyes.....	2
1.3 Aryl and Alkyl Azo Dyes.....	2
1.3.1 Aromatic Azo Dyes.....	2
1.3.2 Aliphatic Azo Dyes.....	3
1.4 General Properties of the Azo Dyes.....	3
1.5 Isomerism in Azo Compounds.....	4
1.5.1 Geometrical Isomerism.....	4
1.5.2 Tautomerisim.....	5
1.6 Synthesis of Azo Dyes.....	5
1.6.1 Diazotization.....	6
1.6.2-Azo Coupling.....	6
1.7 Toxicity of Azo Compounds.....	6
2 EXPERIMENTAL.....	8
2.1 Preparation of the Azo Ligand 2-[2-(5-bromo thiazolylazo)]-4-methoxy phenol (BrTAMP).....	8

2.2 Preparation of Buffer Solutions	10
2.3 Spectral Study of the Reagent BrTAMP	10
2.4 Preparation of BrTAMP Solution	11
2.5 Spectral Study for Complexes.....	11
2.6 Preparation of Standard Metal Ions Solutions	11
2.7 Formation of Mn ⁺ -BrTAMP Complexes	12
2.7.1 Cu (II)-BrTAMP Complex (λ_{\max} =647 nm.)	12
2.7.2 Ni (II)-BrTAMP Complex (λ_{\max} =620 nm.).....	12
2.7.3 Ag (I)-BrTAMP Complex (λ_{\max} =518 nm.)	12
2.8 Optimizing pH for Best Calibration Curve	12
2.8.1 Cu (II)-BrTAMP Complex.....	13
2.8.2 Ni (II)-BrTAMP Complex	13
2.8.3 Ag (I)-BrTAMP Complex.....	13
2.9 The Composition of the Complexes.....	14
2.9.1 Mole Ratio.....	14
2.10 Effect of Temperature	15
2.11 Effect of Time	15
2.12 Precipitation of the Complexes	15
2.13 Molar Conductivity of Metal Complexes	16
2.14 Precision of the Method	16
2.15 Analytical Applications of BrTAMP	16
2.15.1 Determination of Copper (II) in Serum of Human Blood.....	16
2.15.2 Determination of Nickel (II) in Euphrates River (IRAQ-Al-Qadisiya City).....	17
3 RESULT AND DISSCUSION	18

3.1 Synthesis of Reagent 2-[2-(5-bromo thiazolyl) azo]-4 methoxy phenol (BrTAMP).....	19
3.2 Proton NMR Spectrum of Azo Dye BrTAMP.....	19
3.3 Mass Spectrum of Azo Dye BrTAMP	20
3.4 Ultra Violet Spectra	22
3.5 Interpretation of the UV-Visible Spectra in Terms of Electronic Transitions and Magnetic Moments.....	24
3.5.1 Copper (II)-BrTAMP Complex.....	24
3.5.2 Nickel (II)-BrTAMP Complex.....	25
3.5.3 Silver (I)-BrTAMP Complex	25
3.6 Infrared Spectra.....	26
3.7 Determination of the Optimum Conditions	29
3.7.1 Effect of pH.....	29
3.7.2 Effect of Time	31
3.7.3 Temperature Effect.....	32
3.7.4 The Composition of Chelates.....	34
3.7.4.1 Mole Ratio.....	34
3.7.4.2 Jobe's Method	35
3.7.5 Calibration Curve	37
3.8 Molar Conductivity Measurements.....	38
3.9 Calculation of the Metal Complexes Stability Constant (β)	38
3.10 The Proposed Structures for Copper (II), Nickel (II) And Silver (I) BrTAMP Complexes.....	39
3.11 Precision.....	40
3.12 Analytical Application	42

3.12.1 Copper Analysis in Human Blood	42
3.12.2 Ni Analysis in Euphrates River (In Al-Qadesiyia City, Iraq)	42
4 CONCLUSION	44
REFERENCES.....	46

LIST OF FIGURES

Figure 1.1: General Formula of the Azo Dyes.....	2
Figure 3.1: ¹ HNMR Spectrum of Reagent BrTAMP.....	20
Figure 3.2: Mass Spectrum of Reagent BrTAMP.....	22
Figure 3.3: Absorption Spectra of the Reagent (BrTAMP) and Its Ni (II)-complex (1.25×10 ⁻⁴) M in Water-ethanol Solution 50% V/V.....	23
Figure 3.4: Absorption Spectrum of Cu (II)-BrTAMP Complex (1.25×10 ⁻⁴) M in Water-ethanol Solution 50% V/V.....	23
Figure 3.5: Absorption Spectrum of Ag (I)-BrTAMP Complex (1.50×10 ⁻⁴) M in Water-ethanol Solution 50% V/V.....	24
Figure 3.6: Infra Red Spectra of Reagent BrTAMP.....	28
Figure 3.7: Infra Red Spectra of Reagent Cu (II)-BrTAMP Complex.....	28
Figure 3.8: Infra Red Spectra of Ni (II)-BrTAMP Complex.....	29
Figure 3.9: Infra Red Spectra of Ag (I)-BrTAMP Complex.....	29
Figure 3.10: Effect of pH on Absorbance of [Cu (II)-BrTAMP] at 647 nm.....	30
Figure 3.11: Effect of pH on Absorbance of [Ni (II)-BrTAMP] at 620 nm.....	30
Figure 3.12: Effect of pH on Absorbance of [Ag (I)-BrTAMP] at 518 nm.....	31
Figure 3.13: Effect of the Time on Absorbance of [Cu (II)-BrTAMP] at 647 nm. ...	31
Figure 3.14: Effect of the Time on Absorbance of [Ni (II)-BrTAMP] at 620 nm.....	32
Figure 3.15: Effect of the Time on Absorbance of [Ag (I)-BrTAMP] at 518 nm.	32
Figure 3.16: Temperature Effect on the Absorbance Cu (II)-BrTAMP Complex.....	33
Figure 3.17: Temperature Effect on Ni (II)-BrTAMP Complex.....	33
Figure 3.18: Temperature Effect on Ag (II)-BrTAMP Complex.....	34

Figure 3.19: Mole Ratio Method for Absorbance of Cu (II)-BrTAMP at 647nm Versus Ligand to Cu Mole Ratio	34
Figure 3.20: Mole Ratio Method for Absorbance of Ni (II)-BrTAMP at 620 nm Versus Ligand to Ni Mole Ratio.	35
Figure 3.21: Mole Ratio Method for Absorbance of Ag (I)-BrTAMP at 518 nm Versus Ligand to Ag Mole Ratio.	35
Figure 3.22: Jobe’s Method for Absorbance of Cu (II)-BrTAMP at 647 nm.	36
Figure 3.23: Jobe’s Method for Absorbance of Ni (II)-BrTAMP at 620 nm.	36
Figure 3.24: Jobe’s Method for Absorbance of Ag (I)-BrTAMP at 518 nm.	36
Figure 3.25: Calibration Curve for Cu (II)-BrTAMP Complex at 647 nm.	37
Figure 3.26: Calibration Curve for Ni (II)-BrTAMP Complex at 620 nm.	37
Figure 3.27: Calibration Curve for Ag (I)-BrTAMP Complex at 518 nm.	38
Figure 3.28: The Proposed Structural Formula for Cu (II) and Ni (II) Complexes, Where M Represents Cu (II) or Ni (II) ion.	39
Figure 3.29: The Proposed Structural Formula of Ag (I)- BrTAMP Complex.	40

LIST OF SCHEMES

Scheme 1.1: Geometrical Isomerism of Azo Dyes.....	4
Scheme 1.2: Tautomerisim of Azo Dyes.....	5
Scheme 1.3: General Reaction for the Synthesis of Azo Dyes.....	5
Scheme 3.1: Scheme for the Synthesis of the Azo Dye BrTAMP.....	19
Scheme 3.2: MASS-SPEC Fragmentation Route for the Synthesis of the Reagent BrTAMP.....	21

LIST OF TABLES

Table 2.1: Number of Grams of the Complexes that Was Precipitate	15
Table 3.1: Optimum pH, Color, Maximum Absorption Wave Length (nm.), and the Molar Absorptivity of the Complexes.....	18
Table 3.2: Hybridization, Geometry, Transition, Absorption Band Maxima (in cm^{-1} and nm) and Magnetic Moment	26
Table 3.3: Metal: Ligand (M:L), Stability Constant Values (β), Molar Conductivity, Optimal Concentration and Wave Length with Absorption (λ_{max}) of Complexes...	39
Table 3.4: Physical Characteristics of BrTAMP and Its Chelates with Cu, Ni and Ag	43

Chapter 1

INTRODUCTION

The present thesis describe the preparation of new organic reagent 2[2-(5-bromo thiazolyl) azo]-4-methoxy phenol, shortened as BrTAMP, and used for the spectrophotometric determination of trace amount of nickel (II), copper (II), and silver (I) ions. This method is based on the formation of complexes of Ni (II), Cu (II), and Ag (I) ions with BrTAMP. The thiazolyl azo and its derivatives are used in different applications such as an analytical reagent especially in the spectra determination because of high sensitivity and selectivity. Many thiazolyl azo compounds have been synthesized and proposed as highly sensitive chromogenic reagents for the determination of several metal ions and give colored chelating complexes especially with some transition metal ions.

1.1 Azo Dyes

Azo dyes are chemical compounds that have the $R-N=N-R'$ functional group, where R and R' can be either alkyl or aryl group [1]. Azo dyes are derivatives of diimide (also called diazene), $HN=NH$, in which the two hydrogen atoms can be replaced with aliphatic or aromatic groups [2]. The name azo refers to the $N=N$ and is taken from the French name for nitrogen, which is azote. The original word itself is from Greek meaning without "a" life "zoe" [3].

Azo dyes are used in many applications. They are also used as analytical reagents in spectroscopic determination of metals, especially the transition metals, due to their high sensitivity (large absorptivity) and selectivity towards these metals [4].

Approximately 70-80% of all dyes in textile manufacture and food industry are azo dyes. Although azo dyes can provide all the colors of the visible spectrum, in practice the yellow/red dyes are more prominent than the blue/brown dyes [5].

In azo dyes the N=N group bridges and extends the delocalization of the two substituent. This helps to stabilize the N=N group and the long conjugation makes the compounds high absorbing chromospheres, especially to visible light. If both substituent are aromatic, these effects are even more pronounced and the colors are much more vibrant.

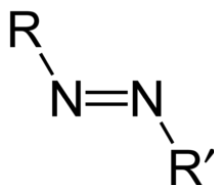


Figure 1.1: General Formula of the Azo Dyes

1.2 Classification of Azo Dyes

Azo compounds (The general formula of the azo dyes is given in Figure 1.1) can be classified according to the number of azo groups that is found in the compound: monoazo for one, diazo for two, or triazo for three azo groups. They can also be classified according to the auxochromic group that is found in it, for example, acidic azo dyes (that have acidic groups such as $-\text{SO}_3\text{H}$, $-\text{COOH}$.) and basic dyes (that have basic groups such as dialylamino, alkylamino and amino.) [6].

1.3 Aryl and Alkyl Azo Dyes

1.3.1 Aromatic Azo Dyes

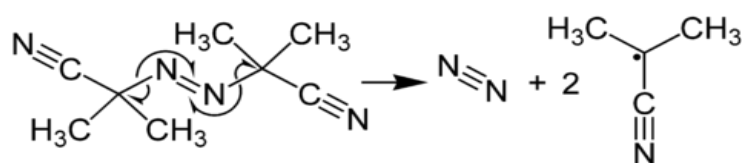
Aromatic azo dyes are generally more stable and tend to be crystalline, such as azobenzene. They are prepared by using a coupling reaction between an aryl cation diazonium and an electron rich nucleophilic aryl ring. These reactions are usually

carried out in an ice bath because diazonium salts tend to be unstable even at room temperature. Azo dyes can be also be made by the oxidation of (R-NH-NH-R') group.

Some azo dyes are harmful and are not manufactured. For example, benzidine derived dyes were discovered to be carcinogenic in the 1980s, and most western countries stopped using them [7, 8].

1.3.2 Aliphatic Azo Dyes

When both substituents are aliphatic, the dyes are called *aliphatic azo* dyes. These are less common as dyes because they have low absorptivity in the visible range and are not stable. For example, diethyl azo (EtN=NtE) breaks into two radicals and to nitrogen gas (sometimes explosively) when irradiated or heated. Thus they can be and are used as radical initiators. A commercially important initiator is Azobisisobutyronitrile (AIBN), whose decomposition results in the formation of two 2-cyanoprop-2-yl radicals [7, 8, 9] as shown below.



1.4 General Properties of the Azo Dyes

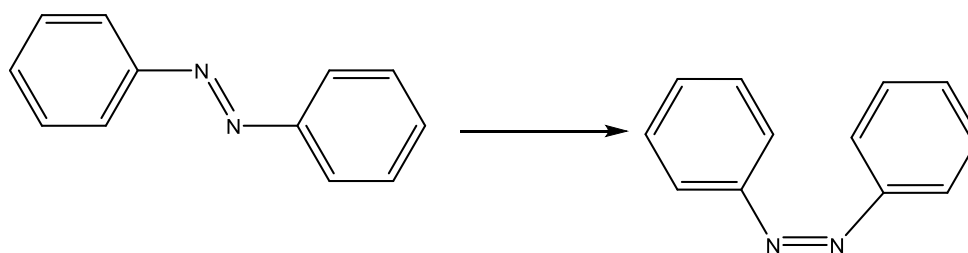
Azo dyes usually have high molar absorptivity in the visible range of the electromagnetic spectrum, and are frequently, intensely and brightly colored. Although they are not as good as the carbonyl and phthalocyanine class of dyes, azo dyes nevertheless possess fairly good fastness. And they are cost-effective because of the way they are manufactured [10].

The general building blocks for any azo dye are a diazo component and a coupling component. Because the starting materials are varied and are readily and cheaply available, the possibility for different azo dyes is very large. Moreover, because the synthesis is easy, it can easily be scaled up or down. This is an important factor for manufacturing cost. The reactions occur at or below room temperature so the energy requirements are low. The environmental impact of the production is minimal because the syntheses are done in water, which is a cheap and plentiful material, with many safe disposal methods. As other classes of dyes become less viable economically as well as for environmental reasons, the attractiveness of azo dyes increase [11].

1.5 Isomerism in Azo Compounds

1.5.1 Geometrical Isomerism

The planar $-N=N-$ bond gives rise to geometrical isomers, namely *trans* and *cis* isomer:



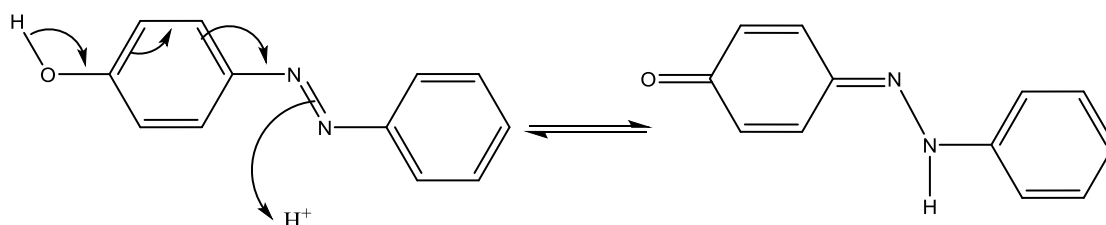
Scheme 1.1: Geometrical Isomerism of Azo Dyes

UV radiation can change the molecule from its preferred *trans* to *cis* conformation. This, sometimes, leads to photochromism, a phenomena where light induces a reversible colour change of the dye. In the past, this effect was considered to be an inconvenience and was prevented by careful development of more stable azo dyes.

However, photochromic dyes have made a comeback on sunroofs, sunglasses, and in the screens of cars [12, 13].

1.5.2 Tautomerism

When a hydrogen atom in a molecule is transported from one part to another, this is called tautomerism [14]. In azo dyes this happens most frequently when a hydroxyl group is present in the para or ortho position as illustrated in Scheme 1.2:

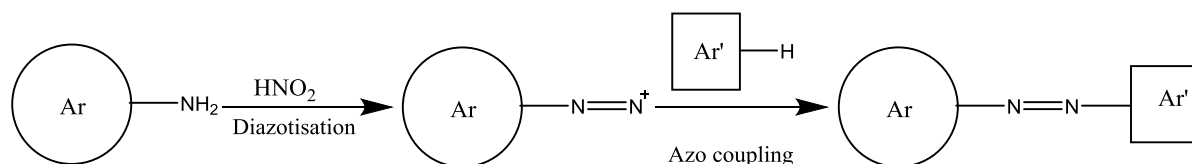


Scheme 1.2: Tautomerism of Azo Dyes.

The forms that result from tautomerism can be identified spectroscopically. The keto-hydrazone absorbs at higher wavelengths than their hydroxyl azo forms. Also keto-hydrazone has larger molar absorptivities. But, tautomerism doesn't occur in all azo compounds, and some tautomeric forms are more stable than the others.

1.6 Synthesis of Azo Dyes

The general synthetic route of azo compounds involves two steps: diazotization and azo coupling. This is shown in Scheme 1.3:



Scheme 1.3: General Reaction for the Synthesis of Azo Dyes

1.6.1 Diazotization

Diazotization is the conversion of a primary aromatic amine to a diazonium cation at low temperature, and in acidic aqueous solution containing nitrous anion, usually added as sodium nitrite with hydrochloric acid [15].

1.6.2-Azo Coupling

The coupling is carried out by treating the unstable diazonium salt in cold aqueous solution with a coupling component such as phenol or an aromatic amine. In this way a stable azo dye is formed [15].

1.7 Toxicity of Azo Compounds

The toxicity of azo compounds is rather low. Furthermore, toxic levels of azo compounds are not usually reached by ingestion of azo dye colored foods. As azo compounds have very low water solubility, they tend not to accumulate in tissue. Generally they are metabolized in the liver and then excreted in urine. Because of their intense color, very little is needed to color foods. So the level of dye addition to food is around a few mg dyes per kg of food. Therefore, an adult would need to eat around 90 kg of azo colored food daily in order to reach dangerous or lethal levels [16].

Yet, there are some azo compounds, intended as food dyes, whose degradation products have shown toxic side effects. These however have been banned from coloring foods.

Enzymes in mammals are able to break down these dyes by attacking the reactive azo linkage. The cleaving and reduction of the azo link splits the molecule into two parts. The enzyme responsible for this reaction is *azoreductase*. It is a non-specific

enzyme, and has been found in all the micro-organisms and mammals that have been tested [17].

Although azoreductase is found in many organs (like kidney, liver, lung, brain, heart, muscles and spleen) in mammals, it shows variable activity. Greatest activity is exhibited by azoreductase in the liver and the kidneys.

The metabolites of azo dyes are absorbed in the intestine and excreted in the urine. The polarity of the azo compounds affect show they are metabolized and excreted. Sulphonated azo compounds appear to be less toxic due to increased excretion in urine. Mono-, di- and trisulphonated compounds are legally used all over the world in foods, drugs and cosmetics [18].

Chapter 2

EXPERIMENTAL

The synthesis, purification and isolation of the ligand 2-[2-(5-bromo thiazolyl) azo]-4-methoxy phenol, shortened as BrTAMP, and preparation of its metal chelates, as well as the various measurements made on the chelate solutions are presented in this chapter.

2.1 Preparation of the Azo Ligand 2-[2-(5-bromo thiazolylazo)]-4-methoxy phenol (BrTAMP)

The new organic reagent BrTAMP was prepared and used for the spectrophotometric determination of copper (II), nickel (II) and silver (I) ions at 10^{-4} M concentration levels. The procedure for the synthesis of the ligand is as follows:-

1- A total of 1.7 g of 2-amino-5-bromo thiazolyl powder form was added to a solution consisting of 20 mL (Analar grade) acetic acid, 5 mL concentrated (Analar grade) hydrochloric acid and 30 mL distilled water in a 500- ml beaker, kept in an ice bath at 0°C.

2- This solution was stirred continuously for 30 minutes until the entire solid dissolved.

3- A total of 0.35 g of sodium nitrate (99%) was placed in 30 mL distilled water in a 100-mL beaker at room temperature. This solution was added drop by drop to the

solution described in step 1, using a burette, and the mixture was stirred continuously for 30 minutes at 0°C in the ice bath.

Immediately upon the addition of sodium nitrate (99% pure) solution to 2-amino-5-bromo thiazole solution, the diazonium chloride was produced (component 1) as observed by the color change of the solution from colorless to light yellow. This color of the diazonium chloride solution changed continuously from light yellow to dark yellow as more of the sodium nitrate was added to the mixture. The solution containing the 2-amino-5-bromo thiazole and sodium nitrate was labeled as component 1.

4- A total of 1.3 g of 4-methoxy phenol in powder form was placed into a solution consisting of 75 mL distilled water and 25 mL (99.98% pure) ethyl alcohol in a 500 - mL beaker at 0°C.

5- A total 1 g of (96% purity) sodium hydroxide was dissolved in 20 mL distilled water in a 25-mL beaker, and then this solution was added to the methoxy phenol solution. This solution was labeled as component 2. This solution was stirred continuously for 30 minutes and kept in an ice bath at 0°C. The color of this solution was dark violet.

6- In the final step of the synthesis, component 2 was added to component 1 drop-wise using a burette. Upon the addition of component 2, the solution began to turn brown in color and gradually a brown precipitate began to form. The brown precipitate is the ligand BrTAMP. The color deepened and the brown precipitate

mass visibly increased as more of the component 2 was added. During the addition, the mixture was stirred continuously at 0°C. After the addition of component 2 was completed, the solution was stirred for a further 30 minutes.

7- This solution was filtered under suction on a Buchner funnel using a Whatman number 41 filter paper. The collected precipitate was washed twice with 2 ml portions water.

The supernatant was allowed to stand for 24 hour, during which more of the product precipitated. This precipitate was also filtered, washed and then combined with the original product that was obtained immediately after the synthesis was completed.

All the brown product which was subsequently shown to be the ligand BrTAMP was placed in a tightly stoppered sample bottle.

2.2 Preparation of Buffer Solutions

Buffer solutions with pH values of 5.0, 5.5, 6.0, 6.5, 7.0, 7.5 and 8.0 were prepared in order to determine the optimum pH medium for the preparation of the metal ion-ligand complexes.

2.3 Spectral Study of the Reagent BrTAMP

The UV-Visible spectrum of the BrTAMP in ethanolic solution and the IR spectrum of the solid BrTAMP were recorded respectively on Shimadzu 1650 double beam UV-visible spectrophotometer using a 1-cm quartz cell, and Shimadzu 8000 FT-IR spectrophotometer in KBr disc.

2.4 Preparation of BrTAMP Solution

Ethanolic BrTAMP solution, based on a molar mass of 314.068 grams, was prepared by dissolving 0.0078 g of BrTAMP in ethanol in a 25 mL volumetric flask. The calculated concentration was [1×10^{-3}] M. Because of its high absorbance value of 1.7 units it was deemed to be too concentrated. Therefore this solution was diluted tenfold to 10^{-4} M, and its absorbance was measured as 0.640 units –a more suitable absorbance value for our experiments.

2.5 Spectral Study for Complexes

The UV-Visible spectrum of the copper (II)-BrTAMP, nickel (II)-BrTAMP and silver(I)-BrTAMP complexes in water-ethanol solution and the IR spectrum of the solid BrTAMP were recorded respectively on Shimadzu 1650 double beam UV-visible spectrophotometer using a 1-cm quartz cell, and Shimadzu 8000 FT-IR spectrophotometer in KBr disc.

2.6 Preparation of Standard Metal Ions Solutions

Three metals solutions with a concentration of 10^{-3} M were prepared using Analar grade 17 mg $\text{CuCl}_2 \cdot 2\text{H}_2\text{O}$, 23 mg $\text{NiCl}_2 \cdot 6\text{H}_2\text{O}$ and 16 mg AgNO_3 and double distilled water in a 25 mL volumetric flask.

As before, absorbance of complex solutions prepared using this solution tended to be very high. Therefore, each metal solution was diluted further to 10^{-4} M. At this concentration absorbance values were more suitable for our experiments.

2.7 Formation of Mn⁺-BrTAMP Complexes

2.7.1 Cu (II)-BrTAMP Complex ($\lambda_{\text{max}}=647$ nm.)

The ligand BrTAMP produces a dark green complex with Cu²⁺ with a maximum absorbance wavelength of 647 nm. The absorbance of the Cu (II)-BrTAMP complex was measured over the concentration range of 10⁻³ to 10⁻⁵ M at 647 nm, in order to determine the optimum working concentration for this complex. An absorbance of about 0.5 was obtained with the 10⁻⁴ M solution. Therefore, subsequent studies were conducted at a concentration of 10⁻⁴ M.

2.7.2 Ni (II)-BrTAMP Complex ($\lambda_{\text{max}}=620$ nm.)

The Ni (II)-BrTAMP exhibits a turquoise color. The absorbance of this complex was also studied over the same concentration range as above, and was found to be optimal at around 10⁻⁴ M concentration with an absorbance of 0.6.

2.7.3 Ag (I)-BrTAMP Complex ($\lambda_{\text{max}}=518$ nm.)

The Ag (I)-BrTAMP had a brown color and it also gave the optimum working concentration as 10⁻⁴ M with an absorbance of 0.7.

2.8 Optimizing pH for Best Calibration Curve

Calibration curves for the concentration range of 0.5 – 1.5 × 10⁻⁴ M complex were prepared at different pH values, in order to determine the optimum pH medium for the complexes. The pH values used were from 5 to 8.5 in steps of 0.5 pH units. The optimum pH that produced the maximum absorbance calibration curve for each metal-ligand complex was selected as the final, working calibration curve for that particular complex. The procedures that were followed are explained below.

2.8.1 Cu (II)-BrTAMP Complex

From the stock Cu (II) and BrTAMP solutions, Cu-Ligand solutions with a 1 to 2 ratio, and an estimated CuL_2 concentration of 0.5×10^{-4} M, 0.75×10^{-4} M, 1.0×10^{-4} M, 1.25×10^{-4} M, 1.5×10^{-4} M were prepared using buffer solution as diluent. The same set of complex solutions were prepared for each of the buffers, from pH=5 to 8.5, in steps of 0.5. The absorbances of these solutions were measured at 647 nm and are plotted in Figure 3.25. From the graph, the optimum pH for absorbance measurements was found to be at pH=6.5. Thus the calibration curve data for the copper-ligand complex was taken from the pH= 6.5 data set.

2.8.2 Ni (II)-BrTAMP Complex

From the stock Ni (II) and BrTAMP solutions, Ni-Ligand solutions with a 1 to 2 ratio, and an estimated NiL_2 concentration of 0.5×10^{-4} M, 0.75×10^{-4} M, 1.0×10^{-4} M, 1.25×10^{-4} M, 1.5×10^{-4} M were prepared using buffer solution as diluent. The same set of complex solutions were prepared for each buffer from pH=5 to 8.5, in steps of 0.5. The absorbances of these solutions were measured at 620 nm and are plotted in Figure 3.26. From the graph, the optimum pH for absorbance measurements was found to be at pH=8. Therefore the calibration curve for the nickel-ligand complex was constructed using the absorbance data for pH=8.

2.8.3 Ag (I)-BrTAMP Complex

From the stock Ag (I) and BrTAMP solutions, Ag-Ligand solutions with a 1 to 2 ratio, and an estimated AgL_2 concentration of 0.5×10^{-4} M, 0.75×10^{-4} M, 1.0×10^{-4} M, 1.25×10^{-4} M, 1.5×10^{-4} M were prepared using buffer solution as diluent. The same set of complex solutions were prepared for buffers from pH=5 to 8.5, in steps of

0.5. The absorbances of these solutions were measured at 518 nm and are plotted in Figure 3.27. From the graph, the optimum pH for absorbance measurements was found to be at pH=7. Hence calibration curve for silver-ligand complex was obtained at pH=7.

2.9 The Composition of the Complexes

The composition of the complexes was examined by the “Mole ratio” and by “Jobe’s” method.

2.9.1 Mole Ratio

Different volumes (0.25, 0.50, 0.75, ..., 3.00) mL of 10^{-3} M BrTAMP solution were placed in 1 mL of 10^{-3} M of M^{n+} solution in a 10-mL volumetric flask individually and diluted with the appropriate (optimum pH) water-ethanol buffer solution for each of the metallic species. Then, the absorbance of each solution was measured at the maximum absorbance wavelength. The absorbance values were then plotted against the mole ratio for each species in order to determine the composition of the complex.

2.9.2 Jobe’s Method

Nine solutions with a final volume of 10 mL were prepared from 10^{-4} M of M^{n+} and 10^{-4} M of BrTAMP solutions. The first solution was prepared with 1 mL of M^{n+} solution and 9 mL of BrTAMP solution, the second with 2 mL of M^{n+} and 8 mL of BrTAMP solution, the third with 3 mL of M^{n+} and 7 mL of BrTAMP solution, etcetera, until the final ninth solution which was 9 mL of M^{n+} solution and 1 mL of BrTAMP. The absorbance of each mixture was measured at the appropriate wavelength.

These absorbance values for each species were plotted on a Jobe’s chart in order to determine the composition of each complex.

2.10 Effect of Temperature

2 mL of 10^{-3} M BrTAMP was placed in 2 mL of 10^{-3} M of M^{n+} solution in a 10-mL volumetric flask, and the volume made up to the mark with water-ethanol solution. Absorbance of this solution was measured at different temperatures. The range of temperatures used was from 0°C to 80°C .

2.11 Effect of Time

2 mL of 10^{-3} M solution was placed in 2 mL of 10^{-3} M of M^{n+} solution in a 10-mL volumetric flask, and the volume made up to the mark with water-ethanol solution. This solution was immediately transferred to a 1 cm cuvette and its absorbance was monitored for 180 minutes.

2.12 Precipitation of the Complexes

Metal-ligand complexes were prepared by adding ethanolic solution of the ligand drop-wise to continuously stirred aqueous solutions of the metal salt. The composition of each solution is given in Table 2.1.

Table 2.1: Number of Grams of the Complexes that Was Precipitate

	<u>BrTAMP solution</u>	<u>Metal salt solution</u>
Cu-BrTAMP	0.75g BrTAMP in 10 mL $\text{C}_2\text{H}_5\text{OH}$	0.211g $\text{CuCl}_2 \cdot 2\text{H}_2\text{O}$ + 10 mL H_2O
Ni-BrTAMP	0.5g BrTAMP in 10 mL $\text{C}_2\text{H}_5\text{OH}$	0.211g $\text{NiCl}_2 \cdot 6\text{H}_2\text{O}$ + 10 mL H_2O
Ag-BrTAMP	0.35g BrTAMP in 10 mL $\text{C}_2\text{H}_5\text{OH}$	0.173g AgNO_3 + 10 mL H_2O

The mixing was carried out at room temperature and after the addition was complete, the mixtures containing the metal-ligand complex were allowed to stand for 24 hours. Each solution was then filtered under vacuum using a Buchner funnel fitted with a Number 41 Whatman filter paper and the precipitate was washed twice with few mL portions of ice-water. The filter paper with the precipitate was allowed to dry

in a desiccator overnight, after which it was collected into a stoppered specimen tube with the aid of a spatula.

2.13 Molar Conductivity of Metal Complexes

A total 0.2 g precipitate of the M^{n+} -BrTAMP complex was placed in two separate 10-mL volumetric flasks. One of the flasks was made up to volume with ethanol (Analar grade) while the other was filled with DMF (Analar grade), all at room temperature. The molar conductivity of each solution was then measured using a conductometer.

2.14 Precision of the Method

The precision of the analytical method was estimated by calculating the standard deviation (S.D) and relative standard deviation (R.S.D) for seven replicate measurements of absorbance for metal-complex solution at optimum concentration, optimum pH and λ_{max} for each metal.

2.15 Analytical Applications of BrTAMP

2.15.1 Determination of Copper (II) in Serum of Human Blood

A 4 mL sample of blood was taken from a worker who was employed in the electricity industry and was suspected of overexposure to copper. The blood sample was placed in 10 mL test tube with 3 mL of aqua regia and the mixture was allowed to stand for 15 minutes (time for complete digestion). After 15 minutes, the solution was centrifuged for about 15 minutes to separate the serum from plasma. After centrifugation, 1 mL of serum was transferred to a 10-mL volumetric flask and 5-sulfosalicylic acid and NaF were added as masking agents, followed by 5 ml of 1×10^{-4} M of BrTAMP to generate the complex. The volume was made up to mark with water-ethanol buffer solution to obtain a final pH of 6.5. The absorbance of this

solution was then measured at the wavelength of 647 nm and the concentration of copper (II) ion in the serum obtained from its calibration graph.

2.15.2 Determination of Nickel (II) in Euphrates River (IRAQ-Al-Qadisiya City)

Six separate samples of water from the Euphrates River in Al-Qadisiya city in Iraq were taken from a depth of 3 meters, at six different locations. From each sample 20 ml portion was taken and placed in a 50-mL beaker; together with 10 mL of concentrated nitric acid, and the solution stirred. This solution was then filtered under suction on a Buchner funnel equipped with a Whatman number 41 filter paper, in order to remove the suspended clay and other particulate matter from the sample. After filtration, the supernatant was transferred quantitatively to a 50-mL volumetric flask, and 5 mL of 0.01 M NaF (99% purity) masking agent, followed by 10 mL 10^{-4} M of BrTAMP were added to the solution. This solution was then made up to the mark with the ethanolic buffer solution to a final pH of 8. Finally, the absorbance of this solution was measured at the maximum absorbance wavelength of 620 nm, and the concentration of Nickel (II) in Euphrates River was determined from the calibration curve for Ni (II).

Chapter 3

RESULTS AND DISCUSSION

Preparation of a novel organic reagent, 2-[2-(5-bromo thiazolyl) azo]- 4-methoxy phenol (BrTAMP) and its use in the spectrophotometric determination of copper (II), nickel (II) and silver (I) at 10^{-4} M concentration levels is described.

The optimum pH for the formation of each metal complex, their color, maximum absorption wavelength and molar absorptivity are given in Table 3.1.

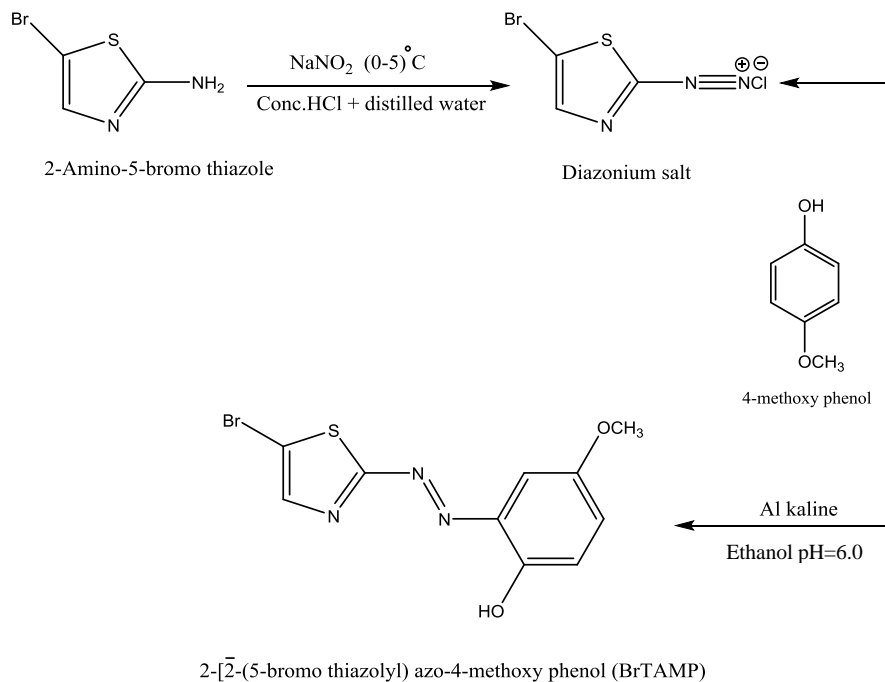
Table 3.1: Optimum pH, Color, Maximum Absorption Wave Length (nm.), and the Molar Absorptivity of the Complexes

Metal Complex	Optimum pH	Color	Maximum absorption wavelength (nm)	Molar Absorptivity, ϵ. (L.mol⁻¹.cm⁻¹)
Copper	6.5	Green	647	3.248×10^3
Nickel	8.0	Turquoise	620	5.544×10^3
Silver	7.0	Brown	518	1.593×10^3

Calibration curve for determining copper (II), nickel (II) and silver (I) conformed to Beer's law in the concentration region 0.50×10^{-4} to 1.50×10^{-4} M as seen in Figures 3.25, 3.26, 3.27 respectively. It may be observed from the analytical data that the metal to reagent ratio (M: L) in copper (II) and nickel (II) to be 1:2; and in silver (I), to be 1:1. Thermal and temporal stability of the complexes were also investigated and are reported here. Statistical treatment of all experimental data is also presented here.

3.1 Synthesis of Reagent 2-[2-(5-bromo thiazolyl) azo]-4 methoxy phenol (BrTAMP)

The azo dye BrTAMP was prepared according to the scheme in Scheme 3.1. The details of the synthesis were given in section 2.1.



Scheme 3.1: Scheme for the Synthesis of the Azo Dye BrTAMP

3.2 Proton NMR Spectrum of Azo Dye BrTAMP

The proton nuclear magnetic resonance spectrum for the reagent (BrTAMP) was obtained in deuterated methanol, CD₃OD, as the solvent. The spectrograph which is reproduced in Figure 3.2 is interpreted as follows:

- 1-Singlet at $\delta=3.755$ ppm corresponding to the three protons in O-CH₃ group.
- 2-Very closely spaced peaks between 7.062 and 7.208 ppm corresponding to the aromatic protons at C3, C5 and C6 of the phenolic ring.
- 3-Singlet at $\delta=8.214$ ppm corresponding the H4 proton on thiazole ring.
- 4-Singlet at $\delta=10.445$ ppm corresponding to the OH proton of the phenol ring.

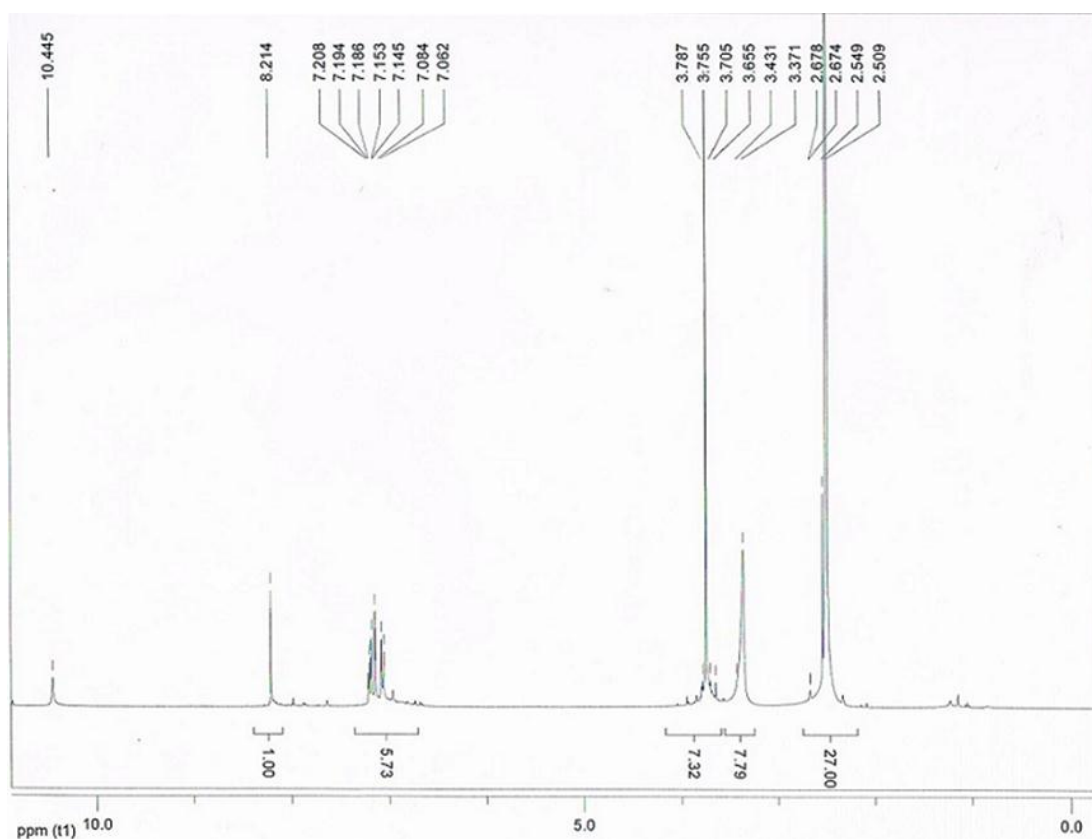
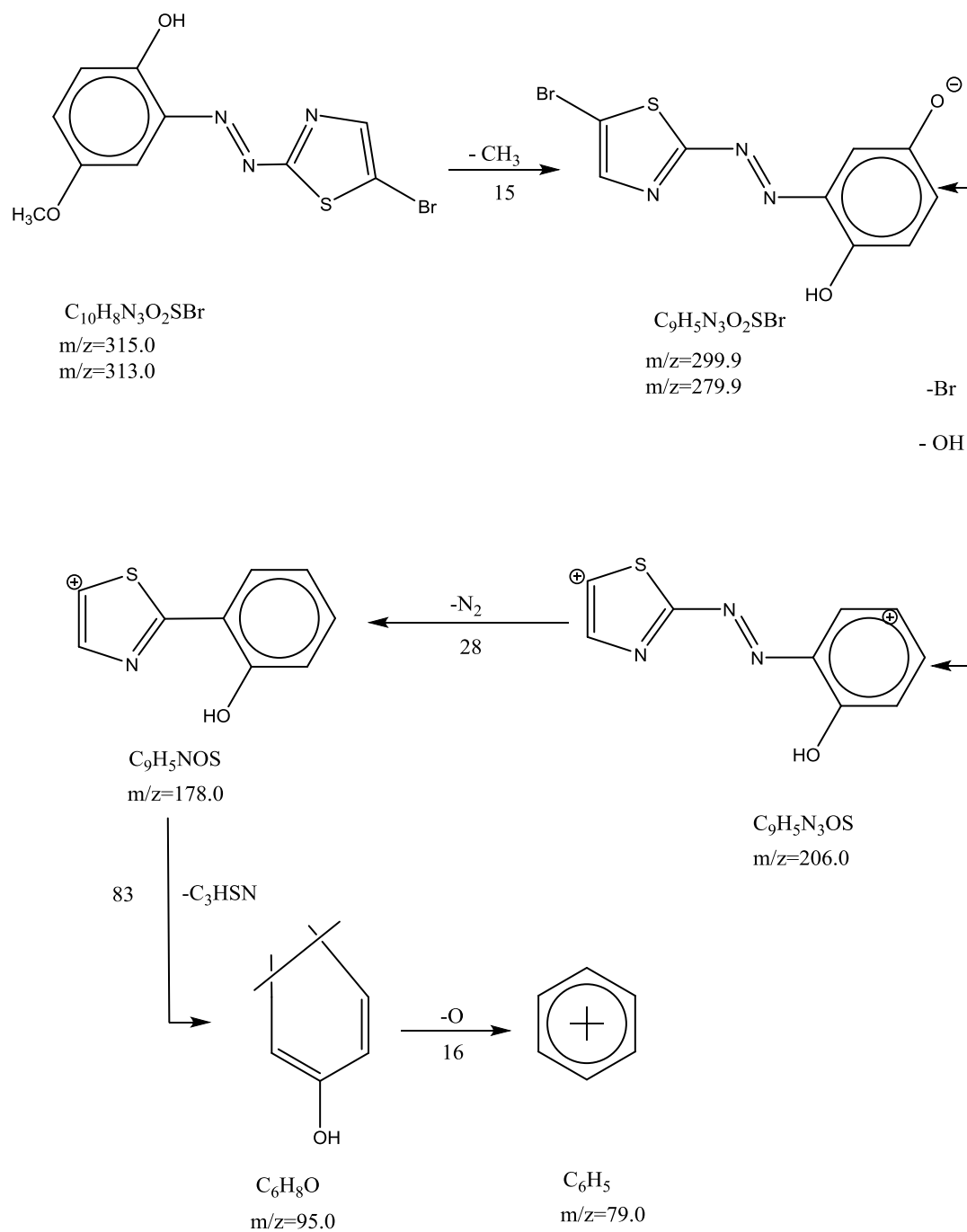


Figure 3.1: ^1H NMR Spectrum of Reagent BrTAMP

3.3 Mass Spectrum of Azo Dye BrTAMP

The mass fragments of azo dye BrTAMP are shown in Figure 3.2. The base peak at $M/Z=$ (315.0 and 313.0) correspond to the molecular ion. The reason for the two peaks with nearly equal intensities is due to the isotopic composition of natural bromine which comprises 50% Br-79 and 50% Br-81. The molecular ion of the reagent with high stability and show the clear peak at (315.0) with relative abundance (100 %) is the emphasis on the health of the molecular structure of the prepared reagent. This reagent takes the route to the mass fragmentation as shown in Scheme 3.2:



Scheme 3.2: MASS-SPEC Fragmentation Route for the Synthesis of the Reagent BrTAMP

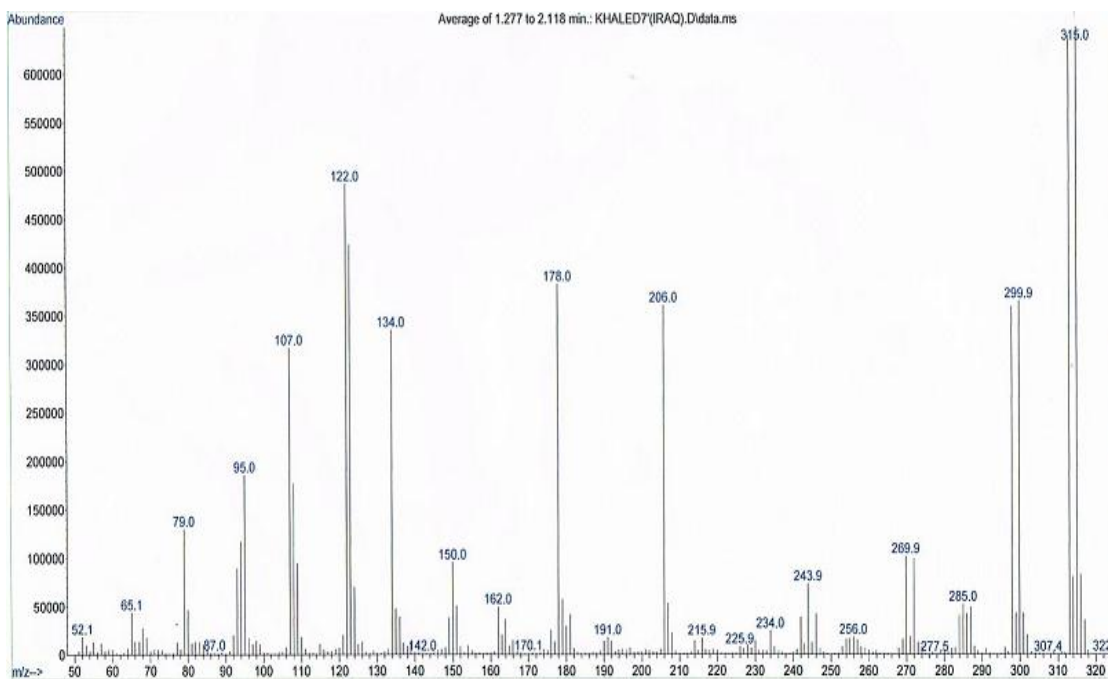


Figure 3.2: Mass Spectrum of Reagent BrTAMP

3.4 Ultra Violet Spectra

U.V spectrum of BrTAMP and its' chelates in absolute ethanol are given in Figure 3.3, 3.4 and 3.5. The maximum absorption (λ_{\max}) wavelength is 488 nm for the free ligand but the metal chelates have absorption maxima (λ_{\max}) at 620 nm for Ni (II)-complex; 647 nm for Cu (II)-complex and 518 nm for Ag (I)-complex. The ligand reacts rapidly with Ni (II), Cu (II) and Ag (I) ions forming turquoise, green and brown complexes, respectively, in water-ethanol solution. In kinetic experiments, it was found that the absorption reached its maximum value within 10 minutes of the addition of ligand to metal solution, and was stable for a minimum of 24 hours at room temperature.

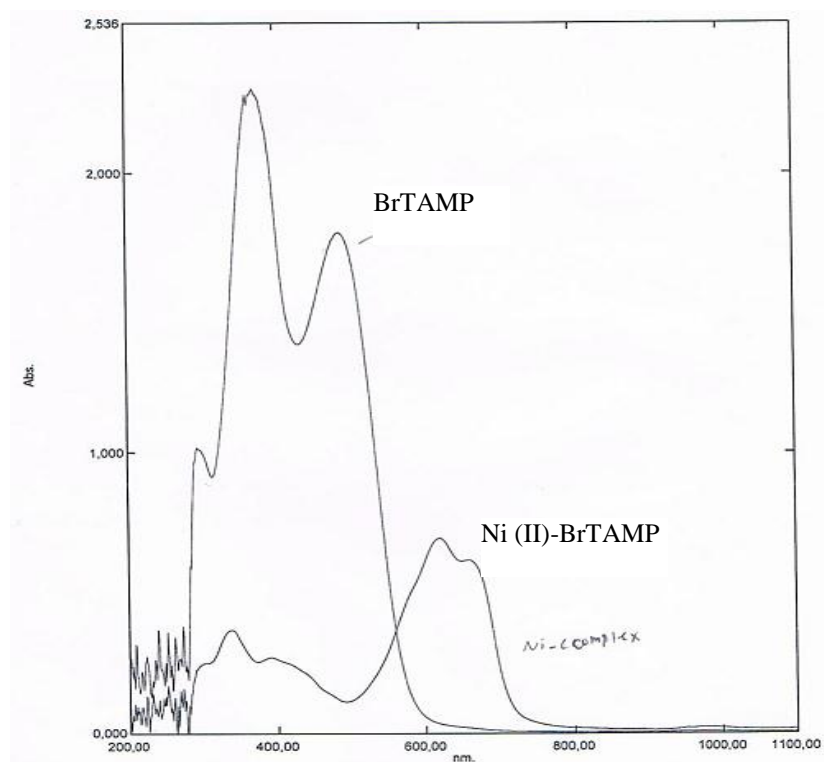


Figure 3.3: Absorption Spectra of the Reagent (BrTAMP) and Its Ni (II)-complex (1.25×10^{-4} M) in Water-ethanol Solution 50% V/V

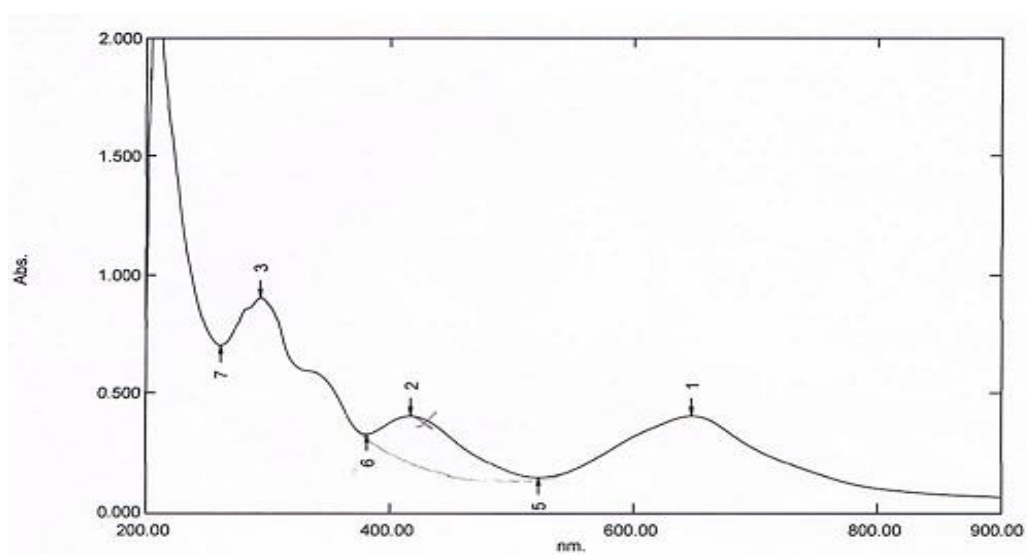


Figure 3.4: Absorption Spectrum of Cu (II)-BrTAMP Complex (1.25×10^{-4} M) in Water-ethanol Solution 50% V/V

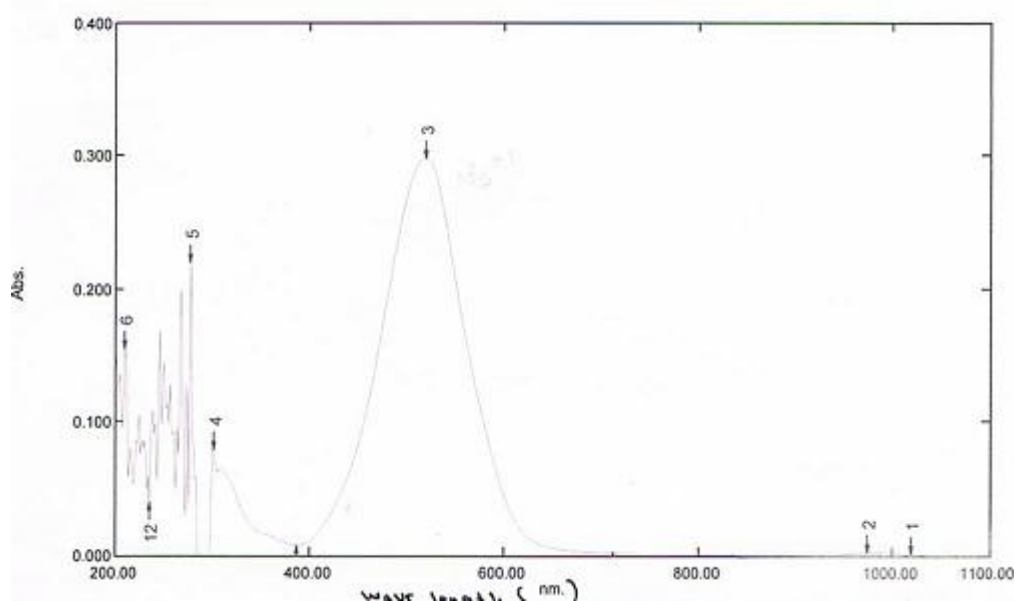


Figure 3.5: Absorption Spectrum of Ag (I)-BrTAMP Complex (1.50×10^{-4}) M in Water-ethanol Solution 50% V/V

3.5 Interpretation of the UV-Visible Spectra in Terms of Electronic Transitions and Magnetic Moments

The electronic spectra of reagent and its complexes were obtained in absolute ethanol solution. The assignment of electronic transition for each spectrum is shown in Table (1). The free BrTAMP data shows three absorption bands. The first band is located at 488 nm (20492 cm^{-1}) for $n-\pi^*$ transition of the azo group ($\text{N}=\text{N}$). This band shifts towards the red-end upon coordination with the metal ion. The second band is 372 nm (26882 cm^{-1}) for $\pi-\pi^*$ transition of the two interacting ($\text{C}=\text{C}$) group of aromatic and thiazole rings, while the third band located at 269 nm (37175 cm^{-1}) is for $n-\sigma^*$ transmission of hydroxyl group (OH) in the aromatic ring.

3.5.1 Copper (II)-BrTAMP Complex

The electronic spectrum of Cu (II)-complex show a broad band at 647 nm (15456 cm^{-1}) which may be assigned to ${}^2\text{E}_g \rightarrow {}^2\text{T}_{2g}$ transition. The magnetic moment value

for this complex was found to be 1.74 B.M due to presence of an unpaired electron. This suggests a distorted octahedral geometry (Z-in or Z-out) and a hybridization of sp^3d^2 [19, 20].

3.5.2 Nickel (II)-BrTAMP Complex

The electronic spectrum of this complex show three absorption bands at 972 nm (10288 cm^{-1}), 659 nm (15174 cm^{-1}) and 620 (16129 cm^{-1}) which are assigned to ${}^3A_2 \rightarrow {}^3T_2g$ (f) (γ_1), ${}^3A_2g \rightarrow {}^3T_1g$ (f) (γ_2) and ${}^3A_2g \rightarrow {}^3T_1g$ (p) (γ_3) transition respectively with an octahedral spatial configuration. The magnetic moment value of the Ni (II)-complex is 3.09 B.M, due to presence of two unpaired electron ($t_2g\ ag^2$), which suggests a high spin octahedral geometry and a hybridization of sp^3d^2 [21].

3.5.3 Silver (I)-BrTAMP Complex

For the Ag (I)-complex, the electronic spectrum did not show any electronic transition (d-d) because they are completely filled with electrons ($4d^{10}$). The absorption band at 518 nm (15305 cm^{-1}) which could be attributed to the presence of a charge transfer ($M \rightarrow L$, CT) complex [22, 23, 24]. The magnetic susceptibility show that this complex has diamagnetic moment ($\mu_{\text{eff}}=0.0\text{ B.M}$) and a tetrahedral geometry hybridization sp^3 .

Table 3.2: Hybridization, Geometry, Transition, Absorption Band Maxima (in cm^{-1} and nm) and Magnetic Moment

Species and Hybridization	Geometry	Transitions	Absorption band maxima		Magnetic Moment B.M
			Wave number (cm^{-1})	Wavelength, λ_{max} (nm)	
BrTAMP	Not applicable	$n \rightarrow \pi^*$	20492	488	
		$\pi \rightarrow \pi^*$	26882	372	
		$n \rightarrow \sigma^*$	37175	269	
[CuL ₂].H ₂ O sp ³ d ² (low spin)	Distorted octahedral	${}^2E_g \rightarrow {}^2T_{2g}$	15456	647	1.74
[NiL ₂].H ₂ O sp ³ d ²	High spin distorted octahedral	${}^3A_{2g} \rightarrow {}^3T_{2g}$ (f) (γ_1)	10288	972	3.09
		${}^3A_{2g} \rightarrow {}^3T_{1g}$ (f) (γ_2)	15174	659	
		${}^3A_{2g} \rightarrow {}^3T_{1g}$ (p) (γ_3)	16129	620	
AgL(H ₂ O) sp ³	Tetrahedral	M → L, CT	15305	518	0.0

3.6 Infrared Spectra

The infrared spectra of azo reagent (BrTAMP) and its complexes with Ni (II), Cu (II) and Ag (I) ions are given in Figures 3.6 , 3.7, 3.8 and 3.9 respectively. These spectra are complex because many of the bands for $\gamma(\text{O-H})$, $\gamma(\text{C=N})$, $\gamma(\text{N=N})$ and other bands for thiazole and phenyl rings in the sub 1700 cm^{-1} region overlap with each other. Position shifts and/or changes in the shapes of the bands in the metal-ligand complexes in comparison to absorption bands for the unbound ligand suggest the possible bonding modes in the complexes. Some of the more significant shifts in the spectra, and the associated interpretations are given below:

1-The spectrum of azo reagent (BrTAMP) shows a broad and medium absorption band around 3422 cm^{-1} due to $\gamma(\text{O-H})$ group. This suggests strong intermolecular hydrogen bonding [25, 26]. In the spectra of Ni (II) and Cu(II) complexes the broad medium absorption bands around $(3439\text{-}3495) \text{ cm}^{-1}$ due to the presence of water in these complexes [27] , but the spectrum of Ag(I) complex show medium absorption band around 3530 cm^{-1} indicates to the coordination water molecule [28, 29].

2-Two weak bands had been observed at 2922 and 3072 cm^{-1} in the reagent spectrum which may be attributed to the aliphatic and aromatic $\gamma(\text{C-H})$, respectively. The positions of the two bands are stable both for BrTAMP and chelates [30].

3-The spectrum of reagent show another band at 1585 cm^{-1} , which is $\gamma(\text{C=N})$ of thiazole ring [31]. This band is observed with a little change in shape and is shifted to lower frequencies (1560-1510) cm^{-1} in the spectra of the complexes. These differences suggest that the metal ions bond via the nitrogen on the thiazole ring [32].

4-Two absorption bands are observed at 1495 cm^{-1} and 1432 cm^{-1} in the BrTAMP spectrum, attributable to lower frequency $\gamma(\text{N=N})$. These bands have been shifted to lower frequencies, 1452 cm^{-1} and 1408 cm^{-1} , with decreased or reduced intensities in the spectrum of the complexes. This may indicates that $\gamma(\text{N=N})$ has been affected by coordination with metal ions [33, 34].

5-The band at 1231 cm^{-1} also appears in the reagent spectrum. This absorption band is due to $\gamma(\text{C-S})$ of thiazole ring. The fixed position of this band in all metal chelates indicates the sulfur atom of heterocyclic ring does not take part in coordination [35, 36]. The absorption bands at (1402, 1275 and 1159) cm^{-1} in free BrTAMP are due to $\gamma(\text{C=C})$, $\gamma(\text{C-O})$ and $\gamma(\text{C=N})$ [37, 38].

6-Finally in the spectra of all chelate complexes there are new bands in the region of 445 to 540 cm^{-1} , which were not present in the free reagent spectrum. This may be attributed to $\gamma(\text{M-O})$ and $\gamma(\text{M-N})$ bands [39, 40]. The infrared spectrum indicates that BrTAMP is a tridentate ligand, which coordinates with the oxygen of the phenyl

group, nitrogen of the N=N group which is closest to the phenyl ring and the nitrogen of thiazole ring, to give two five-membered chelate ring.

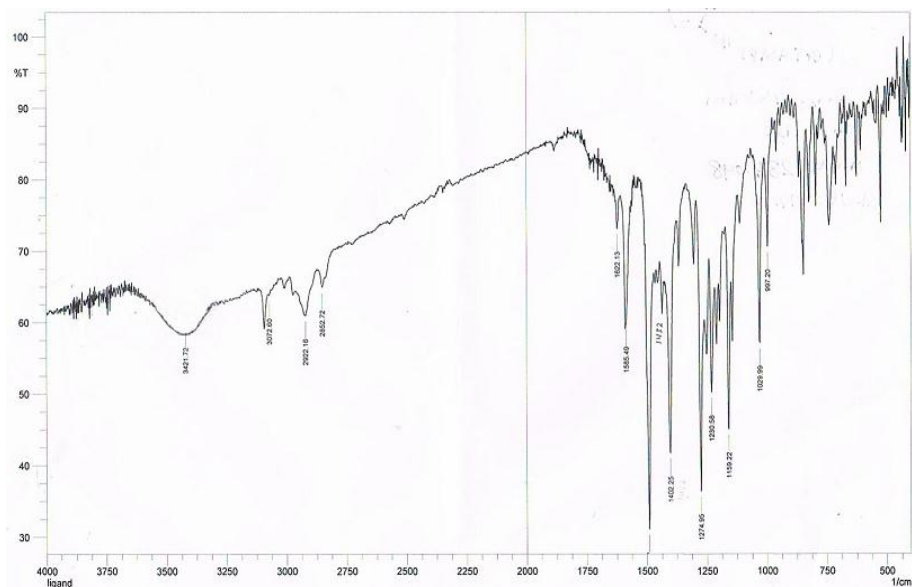


Figure 3.6: Infra Red Spectra of Reagent BrTAMP

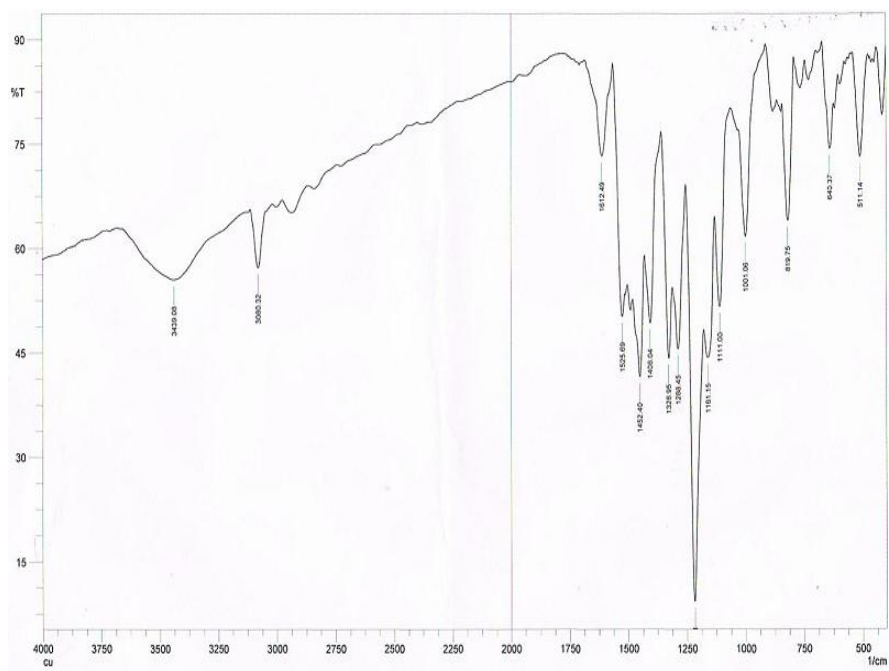


Figure 3.7: Infra Red Spectra of Reagent Cu (II)-BrTAMP Complex

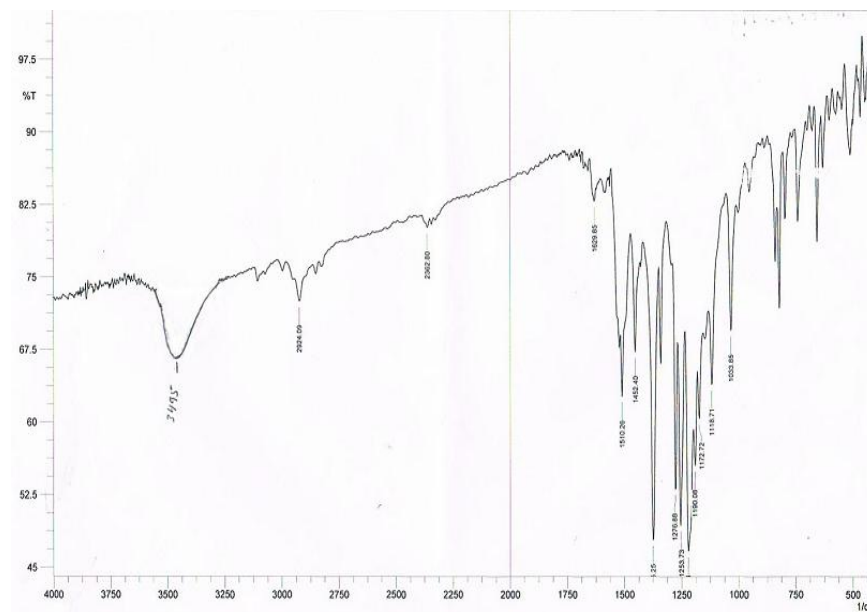


Figure 3.8: Infra Red Spectra of Ni (II)-BrTAMP Complex

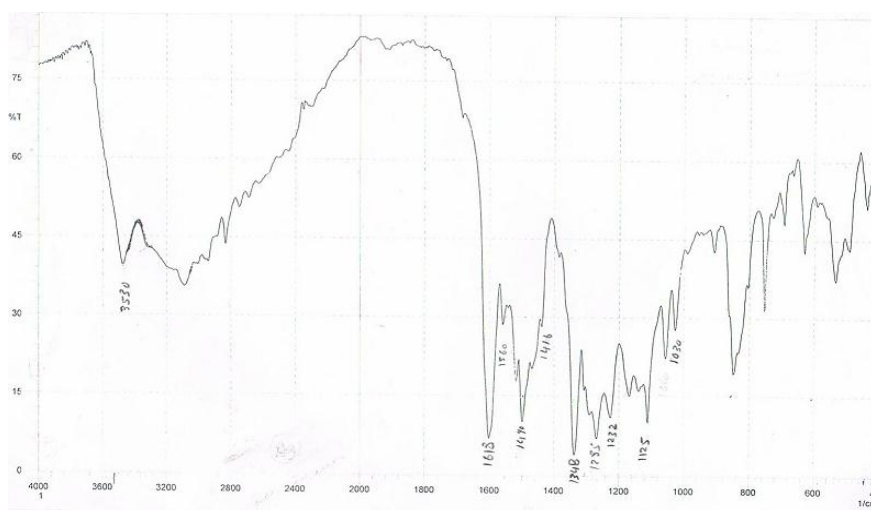


Figure 3.9: Infra Red Spectra of Ag (I)-BrTAMP Complex

3.7 Determination of the Optimum Conditions

3.7.1 Effect of pH

Figures 3.10, 3.11 and 3.12 show that the absorbance of copper (II), nickel (II) and silver (I) complexes measured at λ_{max} change with solution pH. The absorbance of each complex measured at λ_{max} starts low on the acidic side; reaches a maximum at the optimum pH value and then decreases again as pH is increased. The optimum pH

values obtained from the plots give pH=6.5 for Cu (II), pH=8 for Ni (II) and pH=7 for Ag (I). The simplest explanation for these observations is probably that the ligand is highly protonated at low pH, making the nonbonding electron-pairs unavailable and therefore diminishing the tendency to form complexes with the metal cations. On the other hand, when the pH is above the optimum value, hydrolysis of copper (II), nickel (II) and silver (I) ions become more significant and reduce the concentration of the complex [41].

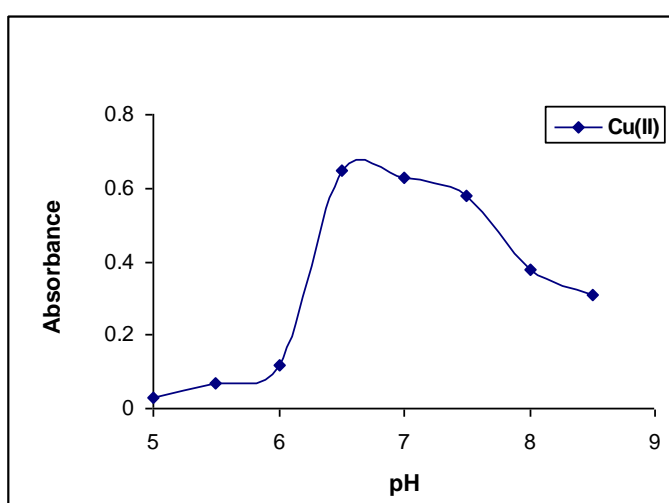


Figure 3.10: Effect of pH on Absorbance of [Cu (II)-BrTAMP] at 647 nm

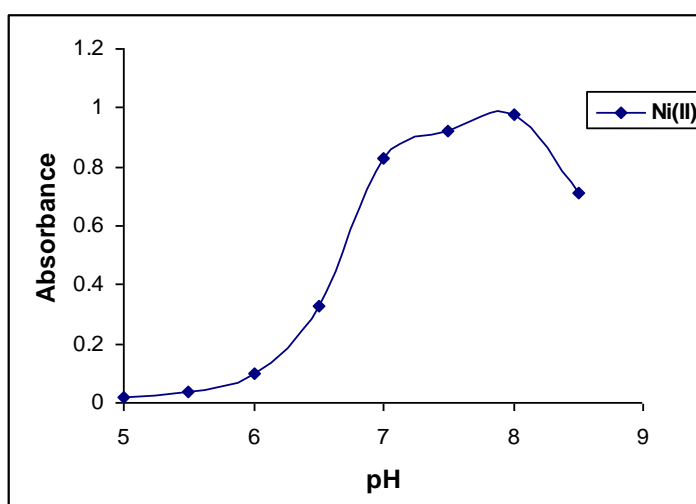


Figure 3.11: Effect of pH on Absorbance of [Ni (II)-BrTAMP] at 620 nm

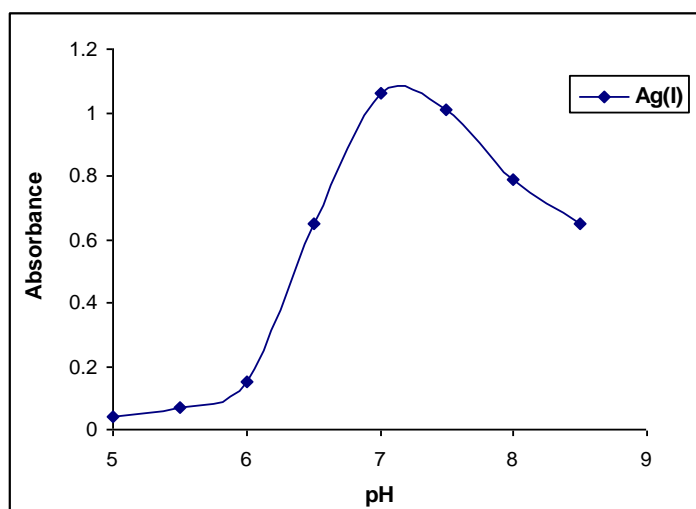


Figure 3.12: Effect of pH on Absorbance of [Ag (I)-BrTAMP] at 518 nm

3.7.2 Effect of Time

When the components are mixed at room temperature, maximum absorbance is reached within 15 minutes. For the duration of the experiment (200 minutes) absorbance remains stable. The ethanolic aqueous solutions of the chelates of Cu (II), Ni (II) and Ag (I) are stable for a minimum of 24 hours. The results are shown in Figures 3.13, 3.14 and 3.15.

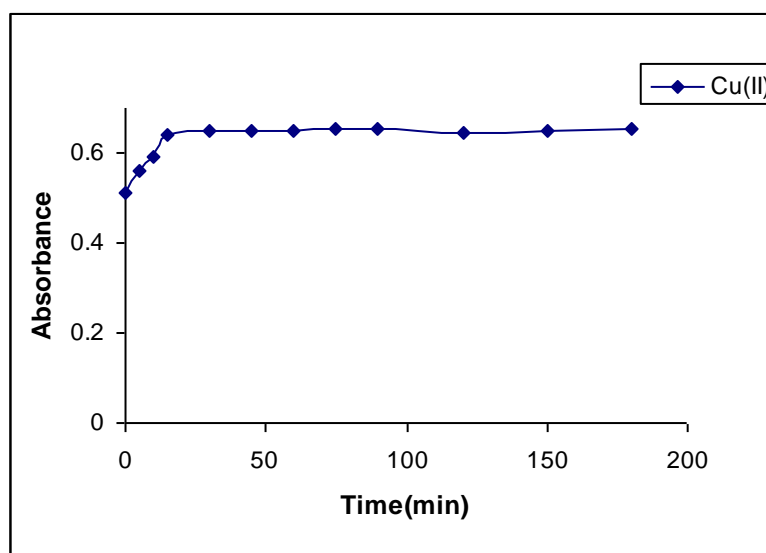


Figure 3.13: Effect of the Time on Absorbance of [Cu (II)-BrTAMP] at 647 nm

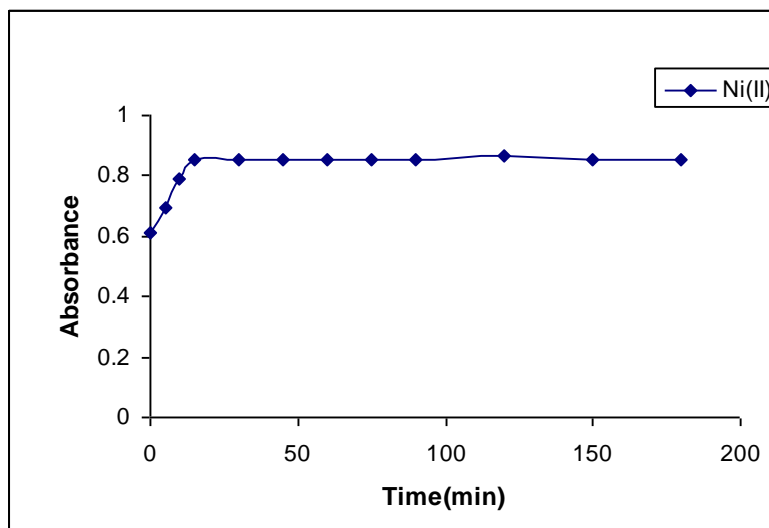


Figure 3.14: Effect of the Time on Absorbance of [Ni (II)-BrTAMP] at 620 nm

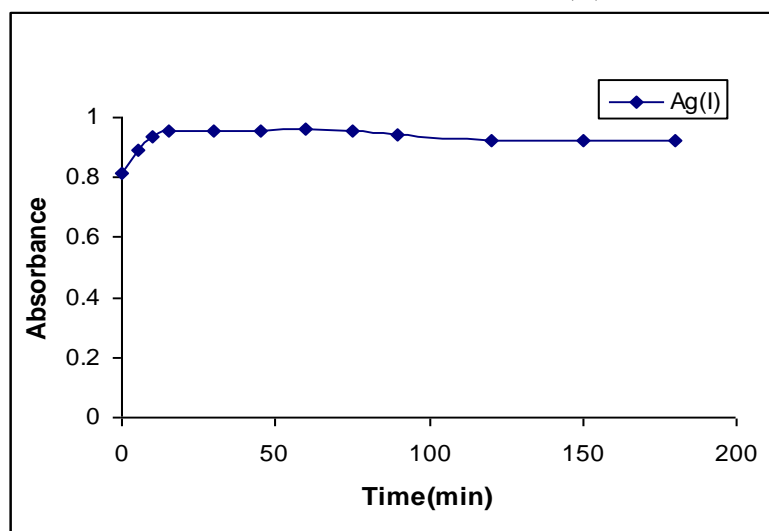


Figure 3.15: Effect of the Time on Absorbance of [Ag (I)-BrTAMP] at 518 nm

3.7.3 Temperature Effect

Temperature effect on the absorptivity of the Cu (II), Ni (II) and Ag (I) complexes were investigated between 10°C and 70°C. In all cases, maximum absorbance was between 20°C and 30°C. Above 35°C, absorbance decreases gradually with increasing temperature. This may be explained by the dissociation of the chelates. The results are shown in Figures 3.16, 3.17 and 3.18.

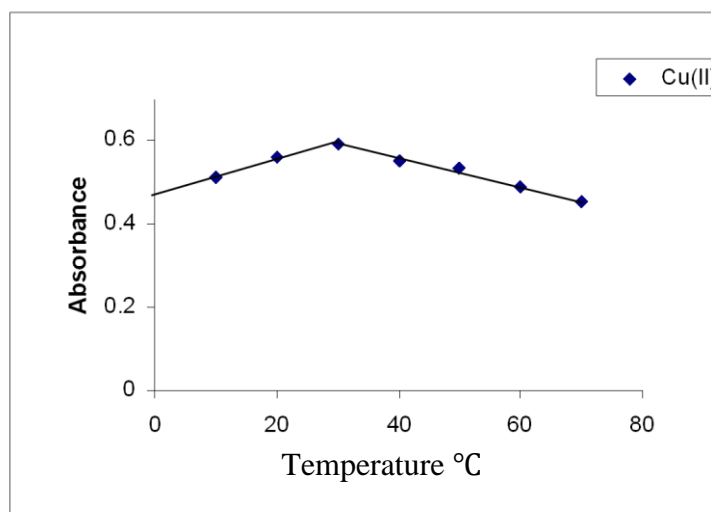


Figure 3.16: Temperature Effect on the Absorbance of Cu (II)-BrTAMP Complex at 647 nm

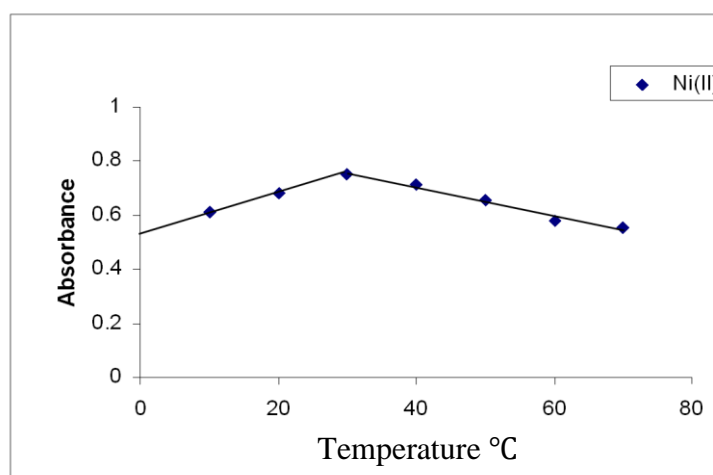


Figure 3.17: Temperature Effect on the Absorbance of Ni (II)-BrTAMP Complex at 620 nm

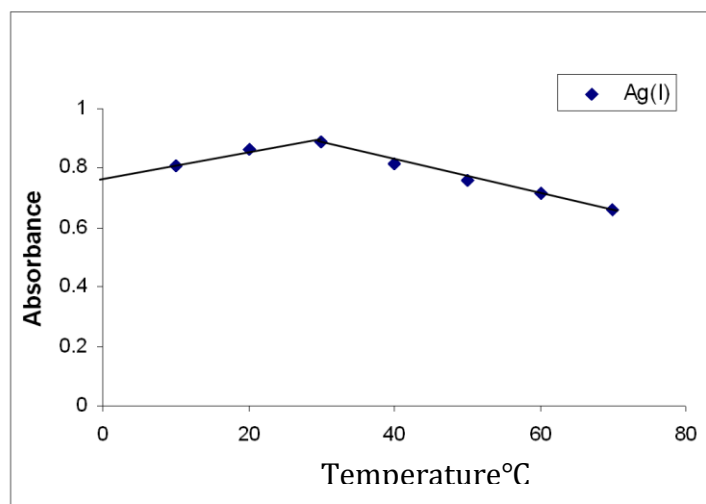


Figure 3.18: Temperature Effect on the Absorbance of Ag (II)-BrTAMP Complex at 518 nm

3.7.4 The Composition of Chelates

The compositions of the chelates were determined by using Jobe's and the mole ratio method.

3.7.4.1 Mole Ratio

This method gave the mole ratio of Cu (II) and Ni (II) ions to reagent BrTAMP as 1:2 (M: L) while for Ag (I) ion as 1:1, as shown in Figures 3.19, 3.20 and 3.21.

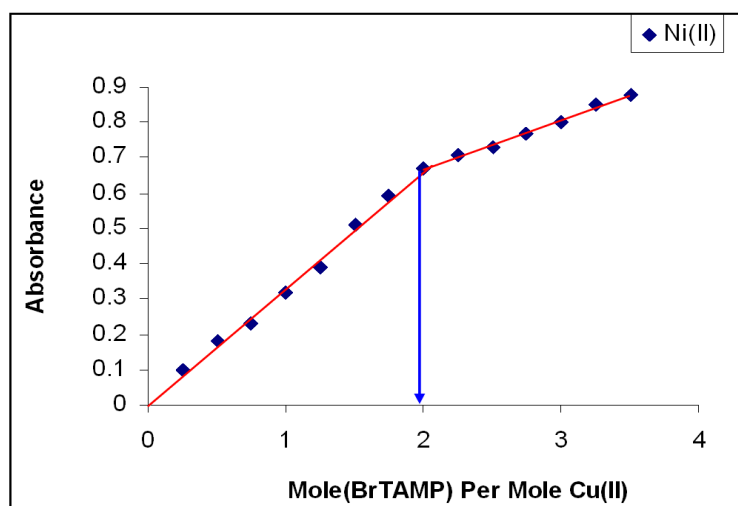


Figure 3.19: Mole Ratio Method for Absorbance of Cu (II)-BrTAMP at 647nm Versus Ligand to Cu Mole Ratio

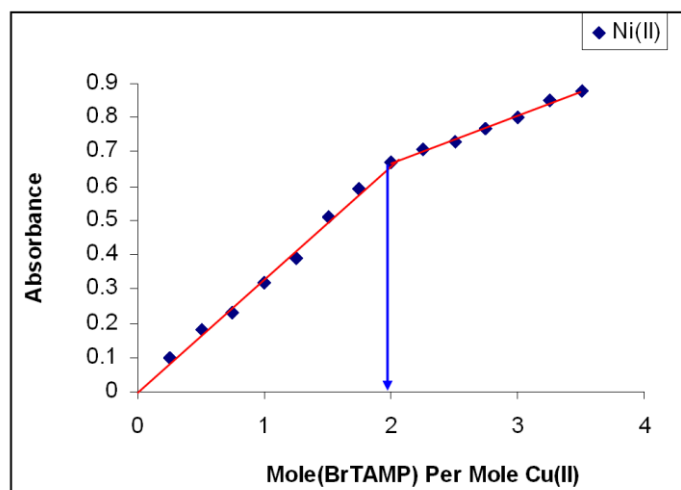


Figure 3.20: Mole Ratio Method for Absorbance of Ni (II)-BrTAMP at 620 nm Versus Ligand to Ni Mole Ratio.

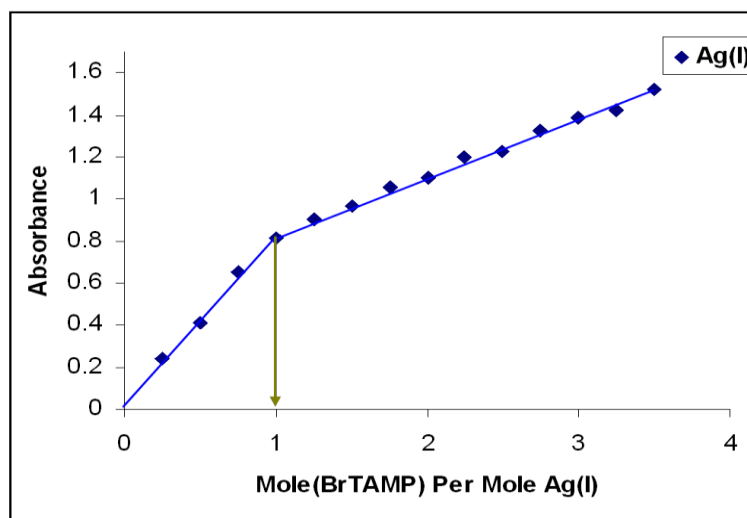


Figure 3.21: Mole Ratio Method for Absorbance of Ag (I)-BrTAMP at 518 nm Versus Ligand to Ag Mole Ratio.

3.7.4.2 Jobe's Method

This method also gave the mole ratio of Cu (II) and Ni(II) ions to BrTAMP as 1:2 (M:L) and the mole ratio for Ag (I) ion to BrTAMP as 1:1. The results are plotted in Figures 3.22, 3.23 and 3.24.

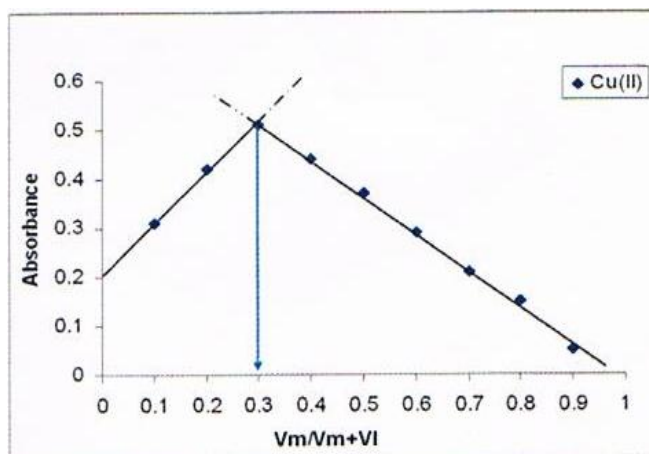


Figure 3.22: Job's Method for Absorbance of Cu (II)-BrTAMP at 647 nm.

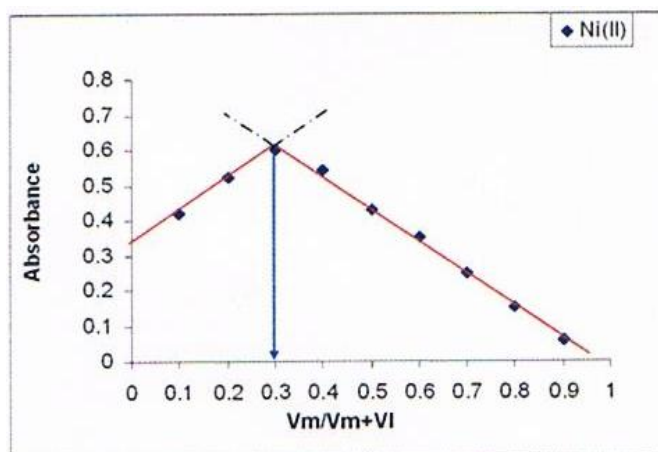


Figure 3.23: Job's Method for Absorbance of Ni (II)-BrTAMP at 620 nm

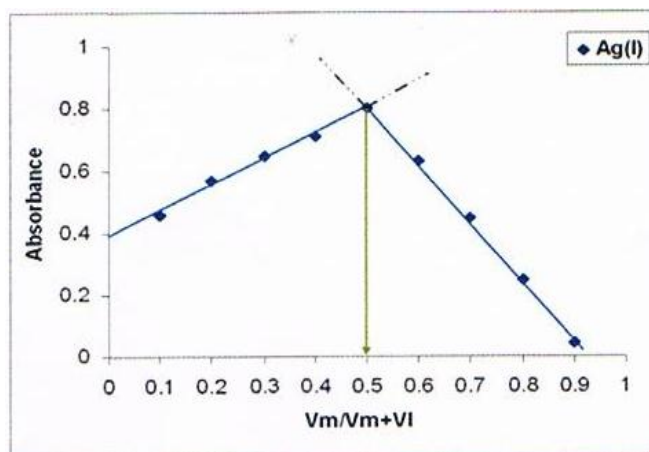


Figure 3.24: Job's Method for Absorbance of Ag (I)-BrTAMP at 518 nm

3.7.5 Calibration Curve

Figures 3.25, 3.26 and 3.27 are the calibration curves for Cu(II), Ni(II) and Ag(I) complexes and they all show good adherence to Beer's Law at the range of concentrations for which the measurements were made. That is, between 0.5×10^{-4} and 1.5×10^{-4} M of the solutions and at the λ_{\max} of each complex (647, 620 and 518 nm for Cu, Ni and Ag respectively) the absorbance varies linearly with concentration.

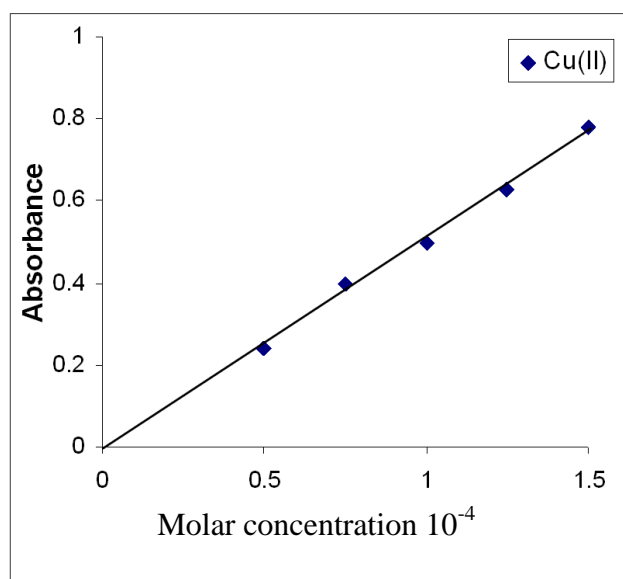


Figure 3.25: Calibration Curve for Cu (II)-BrTAMP Complex at 647 nm

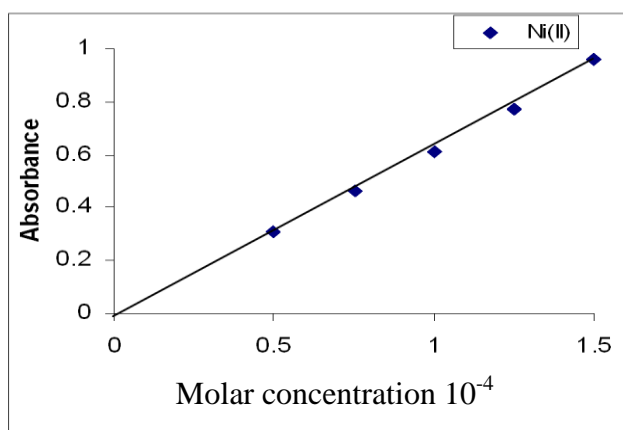


Figure 3.26: Calibration Curve for Ni (II)-BrTAMP Complex at 620 nm.

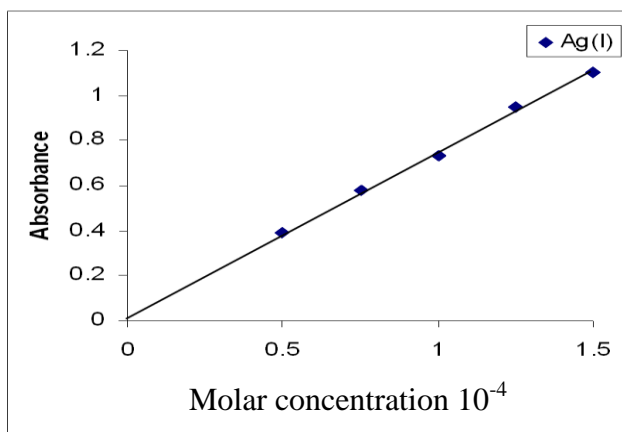


Figure 3.27: Calibration Curve for Ag (I)-BrTAMP Complex at 518 nm.

3.8 Molar Conductivity Measurements

The molar conductivity of the complexes are shown in Table 3.3. Measurements were carried out in ethanol and DMF solvents for complex concentration of 10^{-3} M, at 25°C . Low values for molar conductance indicate that the chelates of Ni (II), Cu (II) and Ag (I) are non or weak electrolytes by nature, and that there are no free anions outside the coordination sphere to carry the current [42, 43].

3.9 Calculation of the Metal Complexes Stability Constant (β)

Stability constant of complexes were obtained spectrophotometrically by measuring the absorbance of solutions of reagent and metal ion at fixed wavelength λ_{max} , and fixed pH. The degree of formation of the complexes were obtained from the relationship proposed by [Vosburgh and Copper], $\beta = (1 - \alpha / 4\alpha^3 C^2)$ for 1:2 (M: L) metal complexes and $\beta = (1 - \alpha / \alpha^2 C)$ for 1:1 (M:L) metal complex and $\alpha = A_m - A_s / A_m$, where A_m and A_s are the absorbance of fully and partially formed complex respectively at optimum concentration[44, 45]. The calculated β values for the complexes are given in table (3.3). The stability constants follows the sequence Ni (II) > Cu (II) > Ag (I). The higher stability of the reagent (BrTAMP) towards Ni (II)

and Cu (II) over Ag (I) indicates to the higher affinity of the ligand to divalent cations [46, 47, 48].

Table 3.3: Metal: ligand (M: L), Stability Constant Values (β), Molar Conductivity, Optimal Concentration and Wave Length with Absorption (λ_{\max}) of Complexes

Reagent	Metal ion	M:L ratio	Optimal molar concentration. $\times 10^{-4}$ M	Optimal wave length λ_{\max} nm	Optimal absorptivity (ϵ) $\times 10^3$ mol.cm $^{-1}$	Molar conductivity S.cm 2 .mol $^{-1}$		β
						EtOH	DMF	
BrTAMP $\lambda_{\max}=488\text{nm}$ $\epsilon = 5.16 \times 10^3$ L.mol $^{-1}$.cm $^{-1}$ Conc= 1.25×10^{-4} M	Ni(II)	1:2	1.25	620	5.544	10.7	13.16	6.87×10^8
	Cu(II)	1:2	1.25	647	3.248	9.56	11.92	5.761×10^8
	Ag(I)	1:1	1.50	518	1.593	8.41	10.39	1.629×10^4

3.9 The Proposed Structures for Copper (II), Nickel (II) And Silver (I) BrTAMP Complexes

From the preceding data, analysis and interpretation, the geometrical structures in Figures 3.28 and 3.29. for the chelates are proposed.

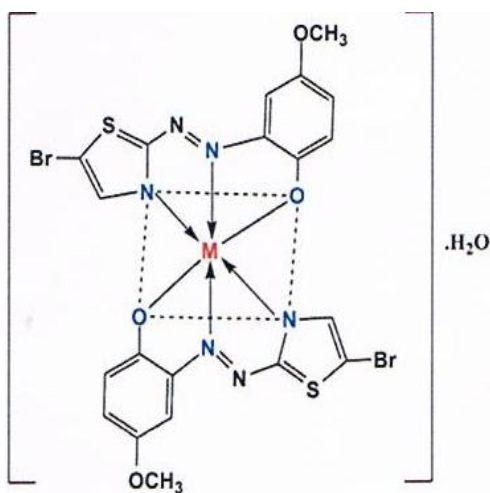


Figure 3.28: The Proposed Structural Formula for Cu (II) and Ni (II) Complexes, Where M Represents Cu (II) or Ni (II) Ion.

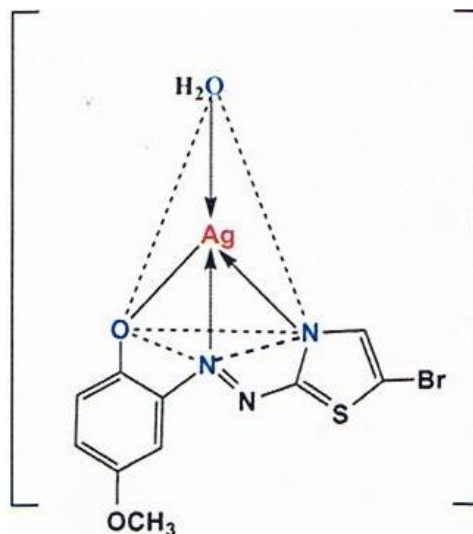


Figure 3.29: The Proposed Structural Formula of Ag (I) - BrTAMP Complex

3.11 Precision

The precision for preparation of complex solutions and measuring their absorbance at λ_{\max} was evaluated by calculating the standard deviation (S.D) and relative standard deviation (R.S.D) for seven replicate samples prepared and measured in an identical way. The data and calculations are tabulated below.

1- Copper (II)-BrTAMP complex

<u>Replicate No.</u>	<u>Absorbance (x_i)</u>
1	0.45
2	0.47
3	0.51
4	0.46
5	0.45
6	0.51
7	0.40
Standard deviation	0.04
Rel. Standard deviation	8.69 %

2-Nickel (II)-BrTAMP complex

<u>Replicate No.</u>	<u>Absorbance (x_i)</u>
1	0.63
2	0.61
3	0.64
4	0.61
5	0.63
6	0.62
7	0.65
<hr/>	
Standard deviation	0.0168
Rel. Standard deviation	2.709%

3-Silver (I)-BrTAMP complex

<u>Replicate No.</u>	<u>Absorbance (x_i)</u>
1	0.68
2	0.67
3	0.70
4	0.68
5	0.69
6	0.64
7	0.66
<hr/>	
Standard deviation	0.0204
Rel. Standard deviation	3.044%

3.12 Analytical Application

3.12.1 Copper Analysis in Human Blood

The amount or concentration of Cu^{2+} present in a sample of human serum was determined by complexing the Cu^{2+} with BrTAMP and measuring its absorbance at 647 nm. The solution tested gave an absorbance of 0.50. This was converted to Cu concentration by use of the calibration curve in Figure 3.25, and was found to be 1×10^{-4} M or 6.4 ppm of Cu^{2+} . When back calculated to the original concentration of Cu in the blood sample, a value of 11 mg/L was obtained. Considering the average concentration of Cu in the literature for human blood is 1-2 ppm [49, 50, 51], and that the sample of blood tested came from an employee in daily contact with Cu metal, the measured quantity appears to be quite reasonable, and substantiates the validity of using BrTAMP as an analytical reagent for the determination of Cu.

3.12.2 Ni Analysis in Euphrates River (In Al-Qadesiyia City, Iraq)

The amount or concentration of Ni^{2+} present in a sample of Euphrates River was determined by complexing the Ni^{2+} with BrTAMP and measuring its absorbance at 620 nm. The value of Ni concentration found appears to be very in high comparison with other data in the literature [52, 53, 54]. The value determined in this method is about 10 ppm while the literature values for Euphrates River are around 0.01 ppm. The discrepancy may be due to the inefficiency in the filtration step. Probably a Whatmann no. 41 filter paper was not sufficiently fine enough to catch all the clay and plankton on the filter and allowed a significant amount to get through. There is therefore a need to repeat this study in a more careful manner ensuring more effective filtration of the river water.

3.13 Some Physical Properties

Table 3.4: Physical Characteristics of BrTAMP And Its Chelates With Cu, Ni And Ag

Compounds	Color	m.p °C	Yield %	Molecular formula (mol.wt) g/mole	Found (cacl.) %				
					C	H	N	S	M
BrTAMP=LH ₂	Brown	143	78	314.068	39.92 (38.16)	2.95 (2.54)	13.85 (13.353)	10.64 (10.18)
[Cu(LH ₂).H ₂ O	Green	174	67	707.8996	34.06 (33.90)	2.23 (2.28)	11.96 (11.87)	9.21 (9.06)	9.14 (8.97)
[Ni(LH ₂).H ₂ O	Turquoise	189	72	702.9996	34.35 (34.14)	2.18 (2.29)	12.10 (11.95)	8.93 (9.12)	9.14 (8.34)
[Ag(LH ₂).H ₂ O	Brown	168	63	439.0322	27.15 (27.36)	2.02 (2.07)	9.71 (9.57)	7.43 (7.30)	24.71 (24.57)

Chapter 4

CONCLUSION

The preparation, identifications and analytical application of the tridentate heterocyclic azo reagent 2-[2-(5-bromo thiazolyl) azo]-4-methoxy phenol, derived from thiazole, is reported in this thesis. The reagent forms water insoluble complexes with Cu (II), Ni (II) and Ag (I) ions. These, however, are readily soluble in ethanol.

The isolated complexes were characterized by spectroscopic and various other analytical techniques. Based on the collected data, the reagent, BrTAMP, was shown to behave as a tridentate ligand, coordinating via the oxygen of phenol, the azo N atom adjacent to methoxy phenol radical, and the thiazol ring nitrogen, to form two five membered metal rings.

The chelation and the subsequent spectrophotometric determination of copper (II), nickel (II) and silver (I) ions in various samples with different matrixes, appears to be simple, quick, selective and sensitive. The Cu (II), Ni (II) and Ag (I) complexes under optimum conditions are stable for at least 24 hours. Stability constants for the Cu (II), Ni (II) and Ag (I) complexes are very high with values of 5.761×10^8 , 6.87×10^8 and 1.629×10^4 L.mol⁻¹ respectively.

The metal ligand ratio (M:L) in alcoholic aqueous solutions as determined by the “mole ratio” and by Jobe's method, both indicate 1:2 for Cu (II) and Ni (II) complexes and 1:1 for Ag (I) complex.

The molar absorptivity for Cu (II), Ni (II) and Ag (I) were found to be 3.248×10^3 at $\lambda_{\max} = 647$ nm, 5.544×10^3 at $\lambda_{\max} = 620$ nm, and 1.593×10^3 at $\lambda_{\max} = 518$ nm, respectively. Beer's law is obeyed in the range of $(0.5 \times 10^{-4} - 1.5 \times 10^{-4})$ M. A distorted octahedral geometry is suggested for Cu (II) and Ni (II) complexes while a tetrahedral is suggested for Ag (I) ion.

The reagent was successfully applied for the determination of copper (II) in human blood serum and nickel (II) in Euphrates River (IRAQ-Al-Qadesiya city).

The strong chelating ability and the high molar absorptivity of the reagent suggest the following possible work for the future.

- i. Solubility of the dye and its metal-chelates may be modified by changing the Br⁻ with more hydrophilic groups. In this way better differentiation in selectivity of the ligand to metals may be achieved in aqueous solutions. Also pH dependent properties may change to permit interference free quantitative determination of metals in presence of each other.
- ii. The ligand may be immobilized on a suitable polymer and its chelating properties utilized for trace metal concentration or removal from dilute solutions.
- iii. The differences in the color of free ligand and chelates may even be used to make visual indicators for particular metals.

REFERENCES

- [1] Nic, M.; Jirat, J.; Kosata, B., eds. (2006–). IUPAC Compendium of Chemical Terminology. <http://goldbook.iupac.org/I03123.html>.
- [2] Eva Engel, Heidi Ulrich, Rudolf Vasold, Burkhard König, Michael Landthaler, Rudolf Süttinger, Wolfgang Bäuml (2008). "Azo Pigments and a Basal Cell Carcinoma at the Thumb". *Dermatology* 216 (1): 76–80.
- [3] Golka K, Kopps S, Myslak ZW (June 2004). "Carcinogenicity of azo colorants: influence of solubility and bioavailability". *Toxicology Letters* 151 (1): 203–10.
- [4] Koh, J. Greaves, A. J. *Dyes Pigments* 2001, 50, 117-119.
- [5] Ramazon, G. Tugba, C. Halil, I. T. *J. Chem.* 2012, 36(1), 66-73.
- [6] Al-Jasser, A. M. *Kuwait Med. J.* 2006, 38, 171-182.
- [7] Ohme, R., Preuschhof, H., Heyne, H.-U. (1988), "Azoethane", Org. Synth., Coll. Vol.6: 78.
- [8] Jean-Pierre Schirmann, Paul Bourdauducq "Hydrazine" in *Ullmann's Encyclopedia of Industrial Chemistry*, Wiley-VCH, Weinheim, 2002.

- [9] (http://en.wikipedia.org/wiki/File:Formation_of_Radicals_from_AIBN.png).
- [10] Chandra, S. Kumar, A. J. Indian Chem. Soc. 2007, 84,325-338.
- [11] Gusev, S. I. Zhvakina, M. V. Kozhevnikov, I. A. Zh. Analit.Khim. 1971, 26, 859-864.
- [12] Ali, A. M. Nat. J. Chem. 2006, 23, 335-343.
- [13] Byabartta, P. Misra, T. K. Sinha, C., Liao, F. L. Panneersel, T. Lu, H. J. Coord. Chem. 2002, 55(5), 479-487.
- [14] Valfredo, A. L. Elenir, S. S. Moacy, S. S., Regino, T. Y. MicroChimica. Acta2007, 158, 189-197.
- [15] Bes, M. W., Kettle, S. F., Powell, D. B. Spectro., Chem., Acta 1974, 30(A), 139-145.
- [16] Colthup, N. B., Daly, L. H., Wiberley, S. E. Introduction.
- [17] W. Manch, and W. C. Fernetins, J. Chem., Educ., 1961, 38. 192.
- [18] W. C. Vosburgh and G. R. Copper; J.Am. Chem., Soc; 1941, 63, 437.
- [19] M.S. Masoud, and Y. H. Abdul-Razek., J. Korean. Chem. Soc., 2002, 46 (2), 99.

- [20] Khalid J. Al-Adilee, and Shayma Adnan; Basrah J, of science (C), 2011, 28 (1), 110.
- [21] B.N. Figgis, and J. Lewis, "Modern Coordination chemistry" Interscience, New York, 1980.
- [22] Khalid J. Al-Adilee and DunyaYo. Fanfon, J. Chem. Chem. Eng., 2012, 6(1), 1016.
- [23] Khalid J. Al-Adilee, Asain Journal of Chemistry, 2012, 24(12), 5597.
- [24] Khalid J. Al-Adilee, Haitham K. and Faiq. F, J. of Al-Qadisia for pure sci., 2011, 16 (2), 50.
- [25] F. A. Snavely, and C.H. Yodeer, J.Org. Chem., 1968, 10, 233.
- [26] A. G. Catchpole, W.B. Foster, and S. Holder, J, spectro chem. Acta, 1962,18,1363.
- [27] H.Bervera, J. Sola, and J.M. Vinas, J. Trans. Met. Chem., 1985, 10, 23.
- [28] A.A.El-Bindary, Transition Met., Chem., 1996, 22, 381.
- [29] A. Z. El-Sonbat and A.A. El. Bindary, Polish. J. Chem., 2000, 74, 621.

- [30] March, J. "Advanced Organic Chemistry" 5th Ed. J. Wiley and Sons, 1992: New York. ISBN 0-471-60180-2.
- [31] S.I. Gusev, M.V. Zhvakina, and I.A. Kozhevnik, J.Zh. Analitkhi, 1971, 26, 659.
- [32] Klaus Hunger, Peter Mischke, Wolfgang Rieper, Roderich Raue, Klaus Kunde, Aloys Engel "Azo Dyes" in Ullmann's Encyclopedia of Industrial Chemistry, 2005, Wiley-VCH, Weinheim.
- [33] L. Mangsup, S. Siripairsarn Pipat, and N. Chaichit, Anal., Sci., 2003, 19, 1345.
- [34] N.B. Colthup, L.H. Daly, and S.E. Wiberley "Introduction to Infrared and Raman Spectroscopy", 2nd Ed. Academic Press.
- [35] B. Singh, R.N. Singh, and R.C. Aggarwal, J. Polyhedron; 1985, 4, 401.
- [36] Y. Saito, C.W. Schlapfer, M. Cordes, and K. Nakamoto, J. Applied Spectra, 1973, 27, 213.
- [37] Khalid J. Al-Adilee, Azhar G. and Ashwaq S. Hussein, J. Chem. Chem. Eng., 2012, 651.
- [38] W.J. Geary, Coord. Chem. Rev., 1971, 17, 81.

- [39] Gung, B.W., Taylor, R.T., 2004. *J. Chem. Ed.*, 81, 1630.
- [40] Decelles, C., 1949, *J. Chem. Ed.*, 26, 583.
- [41] Vogle, A. *I.A Text-Book of Quantitative Inorganic Analysis*, 3rd ed., 1961, pp 512-520.
- [42] Fan, X., Zhang, G., Zhu, C. *Analyst* 1998, 123, 109-117.
- [43] Albert, B., Sussman, M. *Microbiology and Microbial Infections*, 9th ed, Oxford University: New York, 1998.
- [44] H. T. Clarke and W. R. Kirner (1941), "Methyl Red", *Org. Synth., Coll. Vol.1:* 374.
- [45] Clinical and Laboratory Standards, Institute (CLSI), *Performance Standards for Antimicrobial Susceptibility Testing*, 20th in Formational Supplement, M100-520., Wayne Pennsylvania, 30(1), 2010.
- [46] Oyama, H., Ohasin, A. *Anal. Sic.* 2004, 20, 1543-1551.
- [47] Qiu, J., Shen, Y. *J. Mater. Sci.* 2004, 39, 2335-2343.
- [48] Khalid J. Al-Adilee, *Al-Nahrain Univ. J. Sci.*, 2008, 11(3), 31.

[49] Mangsup, L.; Siripaisarnpipat, S.; Chaichit, N. *Anal.Sci.* 2003, 19, 1345-1353.

[50] T. Shanouchi and I. Nakagawa, *J. spectro. Chem., Acta*, 1962, 18, 89.

[51] Raman N. Raja. Y, P., Kulandaisary, *Indian Academy of sci.*, 2001,113(3),183.

[52] isulibrary.isunet.edu/opac/doc_num.php?explnum_id=281.

[53] en.wikipedia.org/wiki/Copper_in_health.

[54] www.readperiodicals.com/201212/2876339841.html.